Table 2
Primers and TaqMan Probes for Genotype Determination

HGF SNPs	Sequence
C(−1652)T (promoter)	
Sense	5′-GGATTAGCAATAGAAACGGGTCAT-3′
Antisense	5′-CCCTGAGGTTGTGGGATATCTAGA-3′
Probe for C(−1652)	Fam-5′-AAAATAGATCCCTCAAAAG-3′-MGB
Probe for T(−1652)	Vic-5′-AATAGATCTCTCAAAAGG-3′-MGB
A43839T (intron 8)	
Sense	5′-TTCAGTAATTTGGGCAGAGTCAGT-3′
Antisense	5′-ACGTTGGTGAAGTCAGCGCTAT-3′
Probe for A43839	Fam-5′-AGTCCAAAAAGTTAGAACT-3′-MGB
Probe for T43839	Vic-5′-AGTCCAAAATGTTAGAAC-3′-MGB
C44222T (intron 9)	
Sense	5′-GCTGGCTTGCAAACAAAATCA-3′
Antisense	5′-GGCTTAGAACTGTGGCTGTCAGT-3′
Probe for C44222	Fam-5′-TTTGAAGCTGGATTTT-3′-MGB
Probe for T44222	Vic-5′-TTGAAGTTGGATTTTT-3′-MGB

were examined for the presence of a polymorphism using Sequencher software (Gene Codes Corporation, Ann Arbor, MI), followed by visual inspection.

2.4. Genotyping of SNPs in the HGF genes

Three SNPs were genotyped using the TaqMan system [14,16]. PCR primers and probes for the TaqMan system are shown in Table 2. Fluorescence level of the reaction products was measured by use of ABI PRISM 7700 or 7900 Sequence Detection System (Applied Biosystems).

2.5. Statistical analysis

Values are expressed as the mean ± S.D. or mean ± S.E. Multiple regression and multiple logistic analyses were performed with the covariates age, body mass index, smoking, current alcohol consumption, presence of diabetes and/or dyslipidemia using the SAS version 6.0 (SAS Institute Inc., Cary, NC). Differences in frequency among the groups were tested by χ^2 analysis. Linkage disequilibrium was evaluated by obtaining r^2 values between polymorphisms using SNPAlyze ver. 2.0 (DYNACOM Co., Ltd., Shigehara, Japan).

3. Results

3.1. Detection of genetic variants in the HGF gene

We systematically searched the sequences obtained for SNPs in 32 volunteer subjects and identified 21 SNPs including 8 SNPs in the HGF promoter, 1 SNP in exon and 12 SNPs in intron regions (Table 3). Ten of these SNPs have been deposited in the public database previously, db SNPs (http://www.ncbi.nlm.nih.gov/SNP/), but 11 of the identified SNPs were novel. Thirteen SNPs had their minor allelic frequency less than 10%, therefore no further studies of these SNPs were undertaken. Six SNPs were in tight linkage disequilibrium, therefore one of them, C44222T, was selected as a representative. Thus, three SNPs, *C(-1652)T*, *A43839T* and *C44222T* were chosen for further genotyping analysis (Table 3).

Table 3
List of 21 Polymorphisms and Alele Frequency in HGF Identified in 32 Japanese Patients by Direct Sequencing

allele 1/allele 2			allele 1		allele 2		allele frequency			
SNPs	aa info.	region	homo	hetero	homo	total	allele 1	allele 2	flanking sequence	dbSNP ID
C(−2142)A		promoter	28	4	0	32	0.938	0.063	ttggaatggggt[c/a]ttatgagctacg	
G(−1965)T		promoter	31	1	0	32	0.984	0.016	atgcctcgcctt[g/t]ggggagaatgaa	
G(−1903)A		promoter	30	1	0	31	0.984	0.016	gctgattctgag[g/a]tcttcatttggg	
C(−1652)T		promoter	10	16	5	31	0.581	0.419	ataaaatagatc[c/t]ctcaaaaggaat	rs3735520
G(−1268)C		promoter	30	1	0	31	0.984	0.016	tctctgaatcaa[g/c]tgaggggtctgg	rs3735521
–(−1215)C		promoter	27	4	0	31	0.935	0.065	taggagtccccc[-/c]atgcccatacaa	
T(−955)C		promoter	31	1	0	32	0.984	0.016	ggacaatgactg[t/c]ttcttggacttt	
T(−578)C		promoter	31	1	0	32	0.984	0.016	aactagacagat[t/c]aggagctggggc	
T40171–*		intron7	0	7	25	32	0.109	0.891	taagtttttttt[t/-]gttgttgttttt	rs5745686
A43839T		intron8	17	14	1	32	0.750	0.250	ctgagtccaaaa[a/t]gttagaactcta	rs2286194
C44222T*		intron9	0	7	25	32	0.109	0.891	ccaagtttgaag[c/t]tggatttttctt	rs2887069
C49065T*		intron9	0	7	25	32	0.109	0.891	acttgtaaaaaa[c/t]cttttgttttta	
T49080C*		intron9	0	7	25	32	0.109	0.891	ttttgttttatc[t/c]gccttgatattc	
A52603G*		intronl0	0	6	26	32	0.094	0.906	cctgttgtttcc[a/g]cagtcatatctt	rs1800793
G58294A		intronl1	31	1	0	32	0.984	0.016	gcctgggtgaca[g/a]aatgagactctg	
T59941A		intron13	31	1	0	32	0.984	0.016	agggcacctggg[t/a]gaggcagtaaaa	rs5745739
T59984G*		intron13	26	6	0	32	0.906	0.094	tgcttgccagac[t/g]gtaagctctgga	rs2074725
G62753T		intron14	31	1	0	32	0.984	0.016	tttgctcttaag[g/t]ttataatatgta	rs5745745
G63555T	Asp543Tyr	exonl5	31	1	0	32	0.984	0.016	agagacttgaaa[g/t]attatgaagctt	
A64588G		intron17	31	1	0	32	0.984	0.016	atgtgaggtaaa[a/g]aggaagttcttt	
T67183G		intron17	31	1	0	32	0.984	0.016	tttaattcctaa[t/g]aatactttgttt	rs5745767

Three SNPs underlined had the minor allele frequency over 10% and were selected for genotyping in this study.
* Six polymorphisms are in strong linkage disequilibrium (r-square > 0.5).

Table 4
Blood Pressure Levels and Carotid Atherosclerosis in Groups Distributed by C(−1652)T Genotypes

Male	CC	CT	TT	*P*
n (%)	519(47.1%)	438(39.7%)	146(13.2%)	
SBP (mmHg)	129.3 ± 0.7	128.8 ± 0.8	129.3 ± 1.4	0.850
DBP (mmHg)	81.4 ± 0.5	80.6 ± 0.5	80.8 ± 0.9	0.355
%Hypertension	41.4	39.0	35.6	0.419
IMT (mm)	0.898 ± 0.005	0.903 ± 0.005	0.892 ± 0.009	0.896
Max-IMT (mm)	1.729 ± 0.035	1.745 ± 0.038	1.650 ± 0.067	0.492
Plaque Score	4.6 ± 0.2	4.9 ± 0.2	4.5 ± 0.3	0.981
Female	CC	CT	TT	*P*
n (%)	579(48.0%)	481(39.9%)	146(12.1%)	
SBP (mmHg)	129.1 ± 0.7	128.8 ± 0.8	127.5 ± 1.5	0.405
DBP (mmHg)	79.0 ± 0.4	79.1 ± 0.5	78.5 ± 0.8	0.727
% Hypertension	35.6	36.0	34.9	0.973
IMT (mm)	0.846 ± 0.004	0.852 ± 0.004	0.848 ± 0.008	0.601
Max-IMT (mm)	1.332 ± 0.021	1.368 ± 0.023	1.371 ± 0.042	0.257
Plaque Score	2.4 ± 0.1	2.6 ± 0.1	2.7 ± 0.2	0.143

SBP: systolic blood pressure, DBP: diastolic blood pressure, IMT: intima-media thickness. Values are mean ± SE.

3.2. Study population

Table 1 shows the clinical characteristics of the present subjects by sex. Most variables (i.e., age, body mass index, diastolic blood pressure, percentage of current alcohol drinking, smoking, diabetes, and hypertension) were significantly higher in men than in women, but percentage of dyslipidemia, serum total cholesterol and HDL cholesterol levels were significantly higher in women than in men. There were no significant differences in systolic blood pressure.

3.3. Association of three polymorphisms with blood pressure and carotid arterioscleorsis

We investigated the possible association of three SNPs in the human *HGF* gene with blood pressure and carotid atherosclerosis in a population-based sample (the Suita Study) that consisted of 2412 participants. The frequencies of each genotype are described in Tables 4-6. The genotype frequencies of all analyzed polymorphisms were consistent with Hardy-Weinberg equilibrium. There were no significant differences in the genotype frequencies of polymorphisms for either sex. Tables also show systolic and diastolic blood pressure levels, and carotid IMT and Plaque Scores in each genotype of the three polymorphisms.

After full adjustment of all confounding factors (age, body mass index, current smoking status, alcohol consumption, presence of diabetes mellitus and dyslipidemia), there was no significant association between the three genotypes and blood pressure levels or the prevalence of hypertension in all subjects and in each sex.

Table 5
Blood Pressure Levels and Carotid Atherosclerosis in Groups Distributed by A43839T Genotypes

Male	AA	AT	TT	*P*
n(%)	555(59.8%)	304(32.8%)	69(7.4%)	
SBP (mmHg)	129.2 ± 0.7	128.4 ± 0.9	130.6 ± 2.0	0.981
DBP (mmHg)	81.3 ± 0.4	80.2 ± 0.6	81.7 ± 1.2	0.550
%Hypertension	38.0	41.1	34.8	0.522
IMT(mm)	0.897 ± 0.005	0.896 ± 0.006	0.888 ± 0.013	0.643
Max-IMT (mm)	1.733 ± 0.034	1.691 ± 0.046	1.743 ± 0.098	0.703
Plaque Score	4.8 ± 0.2	4.4 ± 0.2	4.5 ± 0.5	0.200
Female	AA	AT	TT	*P*
n(%)	636(61.5%)	340(32.9%)	59(5.7%)	
SBP (mmHg)	129.3 ± 0.7	127.4 ± 1.0	131.2 ± 2.3	0.578
DBP (mmHg)	79.0 ± 0.4	78.7 ± 0.5	78.9 ± 1.3	0.790
%Hypertension	36.6	32.1	44.1	0.135
IMT (mm)	0.854 ± 0.004	0.842 ± 0.005	0.837 ± 0.012	0.039
Max-IMT (mm)	1.390 ± 0.021	1.310 ± 0.028	1.232 ± 0.065	0.003
Plaque Score	2.7 ± 0.1	2.3 ± 0.2	1.8 ± 0.4	0.002

SBP: systolic blood pressure, DBP: diastolic blood pressure, IMT: intima-media thickness. Values are mean ± SE.

Table 6
Blood Pressure Levels and Carotid Atherosclerosis in Groups Distributed by C644222T Genotypes

Male	CC	CT	TT	*P*
n (%)	7(0.7%)	194(19.1%)	817(80.3%)	
SBP (mmHg)	125.7 ± 6.2	128.7 ± 1.2	129.3 ± 0.6	0.547
DBP (mmHg)	80.0 ± 3.9	81.2 ± 0.7	80.9 ± 0.4	0.780
%Hypertension	14.2	38.1	40.3	0.334
IMT (mm)	0.895 ± 0.039	0.885 ± 0.008	0.900 ± 0.004	0.096
Max-IMT (mm)	2.066 ± 0.287	1.690 ± 0.057	1.732 ± 0.028	0.856
Plaque Score	2.4 ± 0.9	2.4 ± 0.2	2.5 ± 0.1	0.414
Female	CC	CT	TT	*P*
n (%)	11(1.0%)	207(18.6%)	897(80.5%)	
SBP (mmHg)	130.2 ± 5.3	128.2 ± 1.2	129.1 ± 0.6	0.616
DBP (mmHg)	80.0 ± 3.0	78.2 ± 0.7	79.0 ± 0.3	0.439
%Hypertension	36.4	31.9	37.0	0.383
IMT (mm)	0.825 ± 0.030	0.841 ± 0.007	0.850 ± 0.003	0.161
Max-IMT (mm)	1.317 ± 0.162	1.362 ± 0.036	1.349 ± 0.017	0.844
Plaque Score	6.2 ± 1.5	4.4 ± 0.3	4.8 ± 0.1	0.414

SBP: systolic blood pressure, DBP: diastolic blood pressure, IMT: intima-media thickness. Values are mean ± SE.

Although no association was found between carotid IMT, Plaque Scores and *A43839T* genotype in male subjects, women with the A allele showed significantly thicker IMT and greater Plaque Scores than those with the T allele (Table 5). There was no association between carotid IMT, Plaque Scores and genotypes of the two SNPs, *C(-1652)T* and *C44222T*, in both male and female subjects (Tables 4 and 6).

4. Discussion

Although a number of reports have suggested a strong association between the severity of hypertension and serum HGF levels, there have been few reports that investigated the association between cardiovascular disease and *HGF* gene polymorphisms by direct sequencing. Of those identified single nucleotide polymorphisms, 11 were not deposited in the public database. We have performed a large genetic epidemiological study of the Japanese general population regarding three candidate SNPs in the promoter and intron of the *HGF* gene. There was no significant association between the three *HGF* SNPs and blood pressure or the prevalence of hypertension. Interestingly, female subjects with the A allele of *A43839T* in intron 8 had more severe carotid atherosclerosis than those with the T allele.

4.1. HGF and hypertension, atherosclerosis

Clinical studies have demonstrated a positive correlation between serum HGF concentrations and blood pressure. These studies have gone on to show that serum HGF concentrations in hypertensive patients were significantly higher than those seen in normotensive control subjects [5,6]. In an experimental setting, serum HGF concentrations were significantly increased in spontaneous hypertensive rats compared to Wistar-Kyoto rats at any age, and there was a positive association between serum HGF concentration and blood pressure level [17].

A number of reports have also suggested that serum HGF concentrations are increased in proportion to the development of hypertensive target organ damage. The circulating level of HGF was elevated in patients with myocardial infarction [18] and peripheral arterial disease [9,19,20]. Furthermore, serum HGF concentrations were significantly correlated with the hyperemic response of forearm blood flow and pulse wave velocity [21]. Alternatively, it is apparent that endothelial cell dysfunction may promote abnormal vascular growth, and this vascular remodeling clearly plays an important role in the pathophysiology of atherosclerosis. In normotensive subjects, serum HGF was suggested to maintain the vascular structure and stimulate tissue regeneration in an autocrine-paracrine manner [19,22]. In patients with hypertension or diabetes mellitus, this local HGF system was disturbed by transforming growth factor-β or angiotensin II with the resultant development of abnormal vascular smooth muscle cell growth [17,23].

4.2. HGF SNPs, hypertension, and atheroscleorosis

Polymorphisms of several growth factor genes have been investigated because they may potentially play a key role in the maturation of atheromatous lesions. Among these growth factors, HGF was of particular interest because it could have cardiovascular protective effects in several disorders including hypertension, diabetes mellitus, and cardiovascular diseases.

In the present study, we identified 21 SNPs in the *HGF* gene, and determined the genotype of three of these polymorphisms in more than 2000 individuals. Our results showed that there were no significant associations between *HGF* genotypes and blood pressure levels or the prevalence of hypertension. However, the A allele of *A43839T* in intron 8 was significantly associated with increased severity

of carotid atherosclerosis in females. The reason for this sex-specific effect in our study subjects is unclear. The interaction of HGF with angiotensin II and/or transforming growth factor β could contribute to some of the difference seen in our patients population. Although still controversial [24], renin-angiotensin system related genetic variation tends to appear in male individuals in Japanese [13] and Caucasians [25,26]. Additionally, a T → C transition at nucleotide 869 of the *transforming growth factor β* gene has been reported to be one of the candidate susceptibility loci for hypertension only in the female Japanese population [27]. We assume that there might exist some link or interaction between HGF and the genetic variation of these two growth factors.

Our results suggest that the HGF gene located at chromosome 7q11.2-q21 is a candidate susceptibility locus for atherosclerosis in Japanese women. The polymorphism conferring increased susceptibility for atherosclerosis was located in the intron region without amino acid substitution. Thus, it is possible that the *A43839T* polymorphism in intron 8 of the *HGF* gene is in linkage disequilibrium with some other polymorphisms which are actually responsible for the development of atherosclerosis. To elucidate the exact mechanisms and clinical implications of the association, further functional and linkage disequilibrium analyses are required.

In conclusion, we identified 21 SNPs in the *HGF* gene including 11 SNPs that have never been reported. The present study provides the first evidence that *HGF* may be a candidate susceptibility loci that affects the progression of atherosclerosis in Japanese subjects.

Acknowledgements

We would like to express our highest gratitude to Dr. Soichiro Kitamura, President of the National Cardiovascular Center, for his support of our research. We would like to express our gratitude to Dr. Otosaburo Hishikawa, Dr. Katsuyuki Kawanishi, and Mr. Shigeru Kobayashi for their continuous support of our population survey in Suita city. We also thank the members of the Satsuki-Junyukai. We thank K. Hoshino, Y. Tokunaga, Y. Miyamoto and A. Fukumoto for their technical assistance. This study was supported by the Program for Promotion of Fundamental Studies in Health Science of the Organization for Pharmaceutical Safety and Research of Japan.

References

[1] Nakamura T, Nawa K, Ichihara A. Partial purification and characterization of hepatocyte growth factor from serum of hepatectomized rats. Biochem Biophys Res Commun 1984;122:1450–9.
[2] Morishita R, Aoki M, Nakamura S, Matsushita H, Tomita N, Hayashi S, et al. Potential role of a novel vascular modulator, hepatocyte growth factor (HGF), in cardiovascular disease: characterization and regulation of local HGF system. J Atheroscler Thromb 1997;4:12–9.
[3] Morishita R, Moriguchi A, Higaki J, Ogihara T. Hepatocyte growth factor (HGF) as a potential index of severity of hypertension. Hypertens Res 1999;22:161–7.
[4] Nakamura Y, Morishita R, Higaki J, Kida I, Aoki M, Moriguchi A, et al. Expression of local hepatocyte growth factor system in vascular tissues. Biochem Biophys Res Commun 1995;215:483–8.
[5] Nakamura Y, Morishita R, Nakamura S, Aoki M, Moriguchi A, Matsumoto K, et al. A vascular modulator, hepatocyte growth factor, is associated with systolic pressure. Hypertension 1996;28:409–13.
[6] Nakamura S, Moriguchi A, Morishita R, Aoki M, Yo Y, Hayashi S, et al. A novel vascular modulator, hepatocyte growth factor (HGF), as a potential index of the severity of hypertension. Biochem Biophys Res Commun 1998;242:238–43.
[7] Nishimura M, Ushiyama M, Nanbu A, Ohtsuka K, Takahashi H, Yoshimura M. Serum hepatocyte growth factor as a possible indicator of arteriosclerosis. J Hypertens 1997;15:1137–42.
[8] Yamamoto Y, Kohara K, Tabara Y, Miki T. Association between carotid arterial remodeling and plasma concentration of circulating hepatocyte growth factor. J Hypertens 2001;19:1975–9.
[9] Tateishi J, Waku S, Masutani M, Ohyanagi M, Iwasaki T. Hepatocyte growth factor as a potential predictor of the presence of atherosclerotic aorto-iliac artery disease. Am Heart J 2002;143:272–6.
[10] Weidner KM, Arakaki N, Hartmann G, Vandekerckhove J, Weingart S, Rieder H, et al. Evidence for the identity of human scatter factor and human hepatocyte growth factor. Proc Natl Acad Sci USA 1991;88:7001–5.
[11] Mannami T, Konishi M, Baba S, Nishi N, Terao A. Prevalence of asymptomatic carotid atherosclerotic lesions detected by high-resolution ultrasonography and its relation to cardiovascular risk factors in the general population of a Japanese city: the Suita study. Stroke 1997;28:518–25.
[12] Mannami T, Baba S, Ogata J. Potential of carotid enlargement as a useful indicator affected by high blood pressure in a large general population of a Japanese city: the Suita study. Stroke 2000;31:2958–65.
[13] Higaki J, Baba S, Katsuya T, Sato N, Ishikawa K, Mannami T, et al. Deletion allele of angiotensin-converting enzyme gene increases risk of essential hypertension in Japanese men: the Suita Study. Circulation 2000;101:2060–5.
[14] Ishikawa K, Baba S, Katsuya T, Iwai N, Asai T, Fukuda M, et al. T + 31C polymorphism of angiotensinogen gene and essential hypertension. Hypertension 2001;37:281–5.
[15] Okuda T, Fujioka Y, Kamide K, Kawano Y, Goto Y, Yoshimasa Y, et al. Verification of 525 coding SNPs in 179 hypertension candidate genes in the Japanese population: identification of 159 SNPs in 93 genes. J Hum Genet 2002;47:387–94.
[16] Tanaka C, Kamide K, Takiuchi S, Miwa Y, Yoshii M, Kawano Y, et al. An alternative fast and convenient genotyping method for the screening of angiotensin converting enzyme gene polymorphisms. Hypertens Res 2003;26:301–6.
[17] Nakano N, Moriguchi A, Morishita R, Kida I, Tomita N, Matsumoto K, et al. Role of angiotensin II in the regulation of a novel vascular modulator, hepatocyte growth factor (HGF), in experimental hypertensive rats. Hypertension 1997;30:1448–54.
[18] Zhu Y, Hojo Y, Ikeda U, Shimada K. Production of hepatocyte growth factor during acute myocardial infarction. Heart 2000;83:450–5.
[19] Morishita R, Nakamura S, Hayashi S, Taniyama Y, Moriguchi A, Nagano T, et al. Therapeutic angiogenesis induced by human recombinant hepatocyte growth factor in rabbit hind limb ischemia model as cytokine supplement therapy. Hypertension 1999;33:1379–84.
[20] Yoshitomi Y, Kojima S, Umemoto T, Kubo K, Matsumoto Y, Yano M, et al. Serum hepatocyte growth factor in patients with peripheral arterial occlusive disease. J Clin Endocrinol Metab 1999;84:2425–8.
[21] Komai N, Ohishi M, Morishita R, Moriguchi A, Kaibe M, Matsumoto K, et al. Serum hepatocyte growth factor concentration is correlated with the forearm vasodilator response in hypertensive patients. Am J Hypertens 2002;15:499–506.

[22] Silvagno F, Follenzi A, Arese M, Prat M, Giraudo E, Gaudino G, et al. In vivo activation of met tyrosine kinase by heterodimeric hepatocyte growth factor molecule promotes angiogenesis. Arterioscler Thromb Vasc Biol 1995;15:1857–65.
[23] Nakano N, Morishita R, Moriguchi A, Nakamura Y, Hayashi SI, Aoki M, et al. Negative regulation of local hepatocyte growth factor expression by angiotensin II and transforming growth factor-beta in blood vessels: potential role of HGF in cardiovascular disease. Hypertension 1998;32:444–51.
[24] Sugiyama T, Morita H, Kato N, Kurihara H, Yamori Y, Yazaki Y. Lack of sex-specific effects on the association between angiotensin-converting enzyme gene polymorphism and hypertension in Japanese. Hypertens Res 1999;22:55–9.
[25] O'Donnell CJ, Lindpaintner K, Larson MG, Rao VS, Ordovas JM, Schaefer EJ, et al. Evidence for association and genetic linkage of the angiotensin-converting enzyme locus with hypertension and blood pressure in men but not women in the Framingham Heart Study. Circulation 1998;97:1766–72.
[26] Fornage M, Amos CI, Kardia S, Sing CF, Turner ST, Boerwinkle E. Variation in the region of the angiotensin-converting enzyme gene influences interindividual differences in blood pressure levels in young white males. Circulation 1998;97:1773–9.
[27] Yamada Y, Fujisawa M, Ando F, Niino N, Tanaka M, Shimokata H. Association of a polymorphism of the transforming growth factor-beta1 gene with blood pressure in Japanese individuals. J Hum Genet 2002;47:243–8.

Original Article

Six Missense Mutations of the Epithelial Sodium Channel β and γ Subunits in Japanese Hypertensives

Kei KAMIDE, Chihiro TANAKA*, Shin TAKIUCHI, Yoshikazu MIWA, Masayoshi YOSHII, Takeshi HORIO, Yuhei KAWANO, and Toshiyuki MIYATA*

Liddle's syndrome is an autosomal dominant disease characterized by sodium-sensitive early hypertension and mutations in either the β- or γ-subunit of the amiloride-sensitive epithelial sodium channel encoded by *SCNN1B* and *SCNN1G*. We sequenced the 381 bp-coding regions in exon 13 of *SCNN1B* and the 381 bp-coding regions in exon 12 of *SCNN1G* in 948 and 953 Japanese patients with hypertension, respectively. In the *SCNN1B* gene, we identified three missense mutations, P592S (n=3), T594M (n=2), and E632K (n=1) in a heterozygous state in addition to four synonymous ones, Ile515 (n=1), Ser520 (n=19), Ser533 (n=1), and Thr594 (n=11). In the *SCNN1G gene, we identified* three missense mutations, A578V (n=1), P603S (n=1), and L609F (n=1) in a heterozygous state in addition to two synonymous ones, Ile550 (n=1) and Leu649 (n=91, heterozygous; n=2, homozygous). We did not identify the same mutations previously reported in Liddle's syndrome kindreds. Two of the six hypertensive patients with missense mutation in the *SCNN1B* gene showed atypical renin and aldosterone levels, though one of them was diagnosed with renovascular hypertension. One patient with T594M in the *SCNN1B* gene was resistant to hypertension. The roles of these missense mutations in the *SCNN1B* or *SCNN1G* gene identified in hypertensive patients are not clear in the pathogenesis of hypertension and the regulation of electrolytes. Thus, further investigation of these mutations, including functional analyses, will be needed. (*Hypertens Res* 2004; 27: 333–338)

***Key Words*: Liddle's syndrome, *SCNN1B*, *SCNN1G*, gene variants, hypertension**

Introduction

The amiloride-sensitive epithelial sodium channel (ENaC) is responsible for the rate-limiting step of sodium reabsorption in the distal renal tubules, and thus may play a key role in the maintenance of sodium balance and blood pressure. ENaCs are composed of three homologous subunits, termed α, β, and γ, with a subunit stoichiometry of 2α:1β:1γ (*1*, *2*). These three subunits show a similar topology, consisting of two transmembrane domains separated by a large extracellular domain (*3*). The α-subunit appears to be the conducting unit, and the role of the other two subunits is less certain. Neither the β or the γ subunit, when expressed alone or together, produces any measurable Na^+ current. However, coexpression with the α-subunits greatly enhances the amplitudes of the Na^+ current (*4*, *5*).

Liddle's syndrome is an autosomal dominant disease characterized by sodium-sensitive early hypertension associated with hypokalemic metabolic alkalosis, low plasma renin activity, and suppressed aldosterone secretion. Several mutations have been described in Liddle's kindreds, some in the β subunit and others in the γ subunit (*5*–*7*). All these mutations abolish or modify a highly conserved PY motif present in their intracellular carboxyl terminal region, thereby altering the binding of ENaC to its partner, Nedd4, a ubiquitin-pro-

From the Division of Hypertension and Nephrology and *Research Institute, National Cardiovascular Center, Suita, Japan.

This study was supported by the Program for Promotion of Fundamental Studies in Health Sciences of the Organization for Pharmaceutical Safety and Research of Japan.

Address for Reprints: Kei Kamide, M.D., Ph.D., Division of Hypertension and Nephrology, National Cardiovascular Center, 5-7-1 Fujishirodai, Suita 565-8565, Japan. E-mail: kamide@hsp.ncvc.go.jp

Received September 5, 2003; Accepted in revised form January 24, 2004.

tein ligase (*8–10*). This leads to a low intracellular turnover of the channel and to an increase in the number of active channels exposed at the cell membrane. The underlying hypothesis is that dysregulation of ENaC activity causes inappropriate sodium retention, with consequent volume expansion and suppression of peripheral renin activity in patients with Liddle's syndrome.

Several groups have identified other molecular variants of the β subunit of ENaC (*SCNN1B*) (*11–16*). These variants are missense mutations, and none of them affects the PY motif. Among them, the T594M mutant, which showed a prevalence of 6% to 8% in hypertensives of African descent, was well characterized (*17–20*). Whole cell voltage clamp studies indicated that this variant showed an increased response to cAMP analog (*11, 17*). This mutation has been reported to be the common in black people with essential hypertension in some studies (*18, 19*), but not another (*20*). Some studies have reported that this mutation is common among black individuals with essential hypertension (*18, 19*), but another study found no such association (*20*).

Regarding the γ subunit of ENaC (*SCNN1G*), Iwai *et al.* reported that a single nucleotide polymorphism, G(−173)A, in the promoter region of the *SCNN1G* gene was associated with blood pressure regulation in a Japanese population (*21*). They also showed that the promoter activity of the G(−173) allele was 2- to 3-fold higher than that of the A(−173) allele. This suggests that the γ subunit level is one of the determinants of the ENaC activity. In addition, it suggests that the ENaC activity may be regulated by a subtle change of each subunit protein that could be induced by the missense mutations. As mentioned above, a highly conserved PY motif present in the intracellular carboxyl terminal region of the β and γ subunits of ENaCs is highly important for their regulatory function. This suggests that the surrounding regions—encoded by exon 13 of *SCNN1B* and exon 12 of *SCNN1G*—of the PY motif are also important for the the function of ENaCs.

In the present study, we amplified the 381 bp-coding regions of both exon 13 of *SCNN1B* and exon 12 of *SCNN1G* by polymerase chain reaction (PCR) in 956 Japanese patients with hypertension and successfully sequenced the regions in 948 and 953 patients, respectively. We identified several mutations, including missense mutations, both in *SCNN1B* and *SCNN1G*. Based on our results, we also discuss the clinical profiles of the patients carrying these mutations.

Methods

Subjects

A total of 956 hypertensive subjects (525 men and 431 women; average age: 65.0±10.6 years old; body mass index: 24.2±3.4 kg/m^2) were recruited from the Division of Hypertension and Nephrology at the National Cardiovascular Center; all patients provided their written informed consent to participate in this study.

Ninety-two percent of the study subjects (884 subjects) were diagnosed with essential hypertension, and the rest had secondary hypertension, including renal hypertension (37 subjects), renovascular hypertension (23 subjects), primary aldosteronism (11 subjects) and hypothyroid-induced hypertension (1 subject). The hypertension criteria were blood pressure above 140 and/or 90 mmHg, or the use of antihypertensive agents. The study protocol was approved by the Ethical Review Committee of the National Cardiovascular Center.

Screening of Mutations in the 381 bp-Coding Regions in Exon 13 of the *SCNN1B* Gene and Exon 12 of the *SCNN1G* Gene

Blood samples were obtained from each subject and genomic DNA was isolated from peripheral blood leukocytes by an NA-3000 nucleic acid isolation system (KURABO, Osaka, Japan) (*22*). The 381 bp-coding region in exon 13 of *SCNN1B* was amplified by PCR using a pair of specific primers: 5′-agatggtcacccccctcccgttc-3′ and 5′-taccctcccgaccctt tggagag-3′, which flank the 597-bp region. The 381 bp-coding region in exon 12 of *SCNN1G* was amplified by PCR using a pair of specific primers: 5′-tgcacagagtaagaggaaacagg-3′ and 5′-agcaggctttttggtcagagtat-3′, which flank the 677-bp region. The PCR products were directly sequenced on an ABI PRISM 3700 DNA analyzer (Applied Biosystems, Foster City, USA) as described previously (*23*). The obtained sequences were examined for the presence of a mutation using the Sequencher software package (Gene Codes Corporation, Ann Arbor, USA), followed by visual inspection.

Results

In a total of 956 Japanese patients with hypertension, we screened exon 13 of the *SCNN1B* gene and exon 12 of the *SCNN1G* gene. The 381 bp-coding regions were amplified from the genomic DNA and a total of 948 and 953 sample DNAs were successfully sequenced for *SCNN1B* and *SCNN1G*, respectively. Although we did not identify the same mutations previously reported in Liddle's syndrome kindreds, we identified seven mutations in the *SCNN1B* gene and five in the *SCNN1G* gene. The seven mutations in the *SCNN1B* gene consisted of three missense mutations, one of which has not previously been reported, and four synonymous mutations. The five mutations in the *SCNN1G* gene consisted of three novel missense mutations and two synonymous mutations (Tables 1 and 2).

In *SCNN1B*, three of the 948 individuals had a C-to-T substitution at nucleotide 32053, leading to an amino acid substitution from Pro to Ser at position 592 (P592S). Two of the 948 individuals had a C-to-T substitution at nucleotide 32060, leading to an amino acid substitution from Thr to Met at position 594 (T594M). This T594M mutation was previously identified only in black peoples (*11, 14, 17, 18*).

Table 1. Summary of Sequence Variations of Exon 13 in *SCNN1B* Identified in 948 Japanese Patients with Hypertension

SNP name	Region	Amino acid substitution	Allele 1		Allele 2	Total number	Allele 1	Allele 2
			Homo	Hetero	Homo			
31824C>T	exon13	Ile515Ile	937	1	0	938	0.999	0.001
31839G>C	exon13	Ser520Ser	919	19	0	938	0.990	0.010
31878T>C	exon13	Ser533Ser	940	1	0	941	0.999	0.001
32053C>T	exon13	Pro592Ser	945	3	0	948	0.998	0.002
32060C>T	exon13	Thr594Met	946	2	0	948	0.999	0.001
32061G>A	exon13	Thr594Thr	937	11	0	948	0.994	0.006
32173G>A	exon13	Glu632Lys	947	1	0	948	0.999	0.001

The A of the ATG of the initiator Met codon is denoted nucleotide +1, as recommended by the Nomeclature Working Group (*Hum Mut*, Vol.11, pp.1–3, 1998). The nucleotide sequence (GenBank Accession ID: NT_010604) was used as a reference sequence. *SCNN1B*, β subunit of epithelial sodium channel gene; SNP, single nucleotide polymorphism.

Table 2. Summary of Sequence Variations of Exon 12 in *SCNN1G* Identified in 953 Japanese Patients with Hypertension

SNP name	Region	Amino acid substitution	Allele 1		Allele 2	Total number	Allele 1	Allele 2
			Homo	Hetero	Homo			
28898C>T	exon12	Ile550Ile	952	1	0	953	0.999	0.001
28981C>T	exon12	Ala578Val	952	1	0	953	0.999	0.001
29055C>T	exon12	Pro603Ser	952	1	0	953	0.999	0.001
29075G>C	exon12	Leu609Phe	952	1	0	953	0.999	0.001
29195C>G	exon12	Leu649Leu	860	91	2	953	0.950	0.050

The nucleotide sequence (GenBank Accession ID: NT_010393) was used as a reference sequence. *SCNN1G*, γ-subunit of the epithelial sodium channel gene; SNP, single nucleotide polymorphism.

One of the 948 individuals had a G-to-A substitution at nucleotide 32,173, leading to an amino acid substitution from Glu to Lys at position 632 (E632K). These missense mutations were found in a heterozygous form. In addition, we identified four synonymous mutations (31824C>T: $n=1$; 31839G>C: $n=19$; 31878T>C: $n=1$; 32061G>A: $n=11$) that encoded for Ile515, Ser520, Ser533 and Thr594, respectively (Table 1). Among them, two synonymous mutations (Ser520 and Thr594) were previously reported in Japanese (*13*, *16*, *24*).

In *SCNN1G*, one of the 953 individuals had a C-to-T substitution at nucleotide 28981, leading to an amino acid substitution from Ala to Val at position 578 (A578V). One individual had a C-to-T substitution at nucleotide 29055, leading to an amino acid substitution from Pro to Ser at position 603 (P603S). One individual had a a G-to-C substitution at nucleotide 29075, leading to an amino acid substitution from Leu to Phe at position 609 (L609F). These missense mutations were found in a heterozygous form. In addition, we identified two synonymous mutations (28898C>T: $n=1$; 29195C>G: $n=91$, heterozygous and $n=2$, homozygous) that encoded for Ile550 and Leu649, respectively (Table 2). We also identified two single nucleotide polymorphisms in intron 11, 28732G>A ($n=1$) and 28776G>A ($n=1$).

Tables 3 and 4 show the characteristics of the six patients with missense mutation in *SCNN1B* and of the three patients with missense mutation in *SCNN1G*. An essential hypertensive patient with a missense mutation of P592S in the *SCNN1B* gene (case 1, Table 3) showed high plasma renin activity (PRA; 4.8 ng/ml/h), low plasma aldosterone concentration (PAC; 1.8 ng/dl) and normokalemia (4.3 mEq/l) even while taking β blockade and spironolactone. Both the PRA and PAC in this patient were outside the normal ranges for our institute (normal PRA: 0.2–2.7 ng/ml/h; normal PAC: 2–13 ng/dl) and significantly different from the average values (PRA: 2.1 ng/ml/h; PAC: 15.6 ng/dl) among subjects of the present study who had no secondary hypertension and no missense mutation of the *SCNN1B* or *SCNN1G* genes.

One of the two patients with missense mutation of T594M in the *SCNN1B* gene (case 4, Table 3) showed severe hypertension, with blood pressure of 174/96 mmHg even while taking three kinds of antihypertensive drugs (calcium channel blockade, angiotensin II receptor antagonist and α1-adrenergic blocker).

One patient with missense mutation of E632K in the *SCNN1B* gene and renovascular hypertension (case 6, Table 3) showed much greater levels of both PRA (22 ng/ml/h) and PAC (102.9 ng/dl) compared to the other subjects with renovascular hypertension (average PRA: 6.9 ng/ml/h; average PAC: 18.7 ng/dl), as well as clear hypokalemia (2.7 mEq/l) despite spironolactone therapy.

Other hypertensive patients with missense mutations in

Table 3. Clinical Profiles of Hypertensives with Missense Mutations in Exon13 of *SCNN1B*

	Case					
	1	2	3	4	5	6
Polymorphism	Pro592Ser	Pro592Ser	Pro592Ser	Thr594Met	Thr594Met	Glu632Lys
Age (years old)	62	73	67	58	91	66
Sex	male	male	female	female	female	female
BMI (kg/m^2)	28.2	26.3	22.8	28.5	25.6	20.5
Diagnosis	EHT, NIDDM, HL, OMI	EHT, HL, EA	EHT, NIDDM, HL	EHT, NIDDM, HL	EHT, HL, OCI	RVHT, IGT, HL, ASO, OCI
HT duration (years)	30	20	11	23	50	11
HT family Hx	father	mother	none	brother	mother, brother	none
SBP (mmHg)	140	138	150	174	122	150
DBP (mmHg)	88	70	80	96	62	70
Medication	CCB, BB, spironolactone	CCB	CCB	CCB, ARB, AB	CCB, BB	CCB, ARB, spironolactone
Na (mEq/l)	137	138	139	140	142	142
K (mEq/l)	4.3	4.9	3.9	4.4	4.4	2.7
Cl (mEq/l)	101	109	100	102	108	98
Creatinine (mg/dl)	0.8	0.9	0.3	0.5	0.9	1.2
Overt proteinuria	−	−	−	+	−	+
PRA (ng/ml/h)	4.8	no data	1.1	0.8	1.4	22
PAC (ng/dl)	1.8	no data	8	22.6	9.3	102.9
FBS (mg/dl)	109	89	143	110	108	106
HbA1c (mg/dl)	7.2	5.3	8.0	5.3	5.6	5.7

SCNN1B, β-subunit of epithelial sodium channel gene; BMI, body mass index; EHT, essential hypertension; NIDDM, non-insulin dependent diabetes mellitus; HL, hyperlipidemia; OMI, old myocardial infarction; EA, effort angina; OCI, old cerebral infarction; RVHT, renovascular hypertension; IGT, impaired glucose tolerance; ASO, atherosclerotic obliterance; HT, hypertension; Hx, history; SBP, systolic blood pressure; DBP, diastolic blood pressure; CCB, calcium channel blocker; BB, β-adrenergic blocker; ARB, angiotensin II receptor blockade; AB, α1-adrenergic blocker; PRA, plasma renin activity; PAC, plasma aldosterone concentration; FBS, fasting blood sugar.

SCNN1B (cases 2, 3, 5, Table 3) and *SCNN1G* (cases 1–3, Table 4) did not show specific abnormalities of electrolytes, renin and aldosterone levels, or renal function.

Discussion

By the direct DNA sequence method, we determined the DNA sequence of the 381 bp-coding region in exon 13 of the *SCNN1B* gene and of the 381 bp-coding region in exon 12 of the *SCNN1G* gene in 948 and 953 Japanese patients with hypertension and identified seven and five mutations, respectively. Several previous studies have screened for mutation in exon 13 of the *SCNN1B* gene using the single-strand conformational polymorphism (SSCP) method (*11–13*, *15*, *16*). SSCP is highly sensitive for detecting polymorphism (*25*). We adopted the direct DNA sequence method instead of the SSCP method, because it is more accurate than the SSCP method. A screening of mutations by sequencing was previously performed in a large Japanese cohort including 90 hypertensives and 51 controls (*24*). In that study, however, the authors only sequenced a part of *SCNN1B* and none of *SCNN1G*. Therefore, our study is the first complete, large-scale screening effort to detect mutations in the coding region of exon 13 of the *SCNN1B* gene and exon 12 of the *SCNN1G* gene, *i.e.*, in the regions where the causative mutations of Liddle's syndrome are located.

Among the three missense mutations we identified in exon 13 of the *SCNN1B* gene, the P592S mutation was previously identified in four out of 803 Japanese subjects by SSCP screening followed by DNA sequencing (*13*). It has been reported that this missense mutation was not associated with either home or casual blood pressure values. Although we were not able to determine whether this P592S mutation in the *SCNN1B* gene was associated with blood pressure elevation in the present study, since all our subjects were hypertensive, one essential hypertensive patient with the P592S mutation showed high PRA, low PAC, and normokalemia, even though he was taking β blockade and spironolactone.

The T594M mutation we identified in the *SCNN1B* gene was originally reported in 6.1% of African-American subjects but not seen in Caucasians (*11*). In other studies, this mutation was not observed in Japanese individuals (*13*, *14*). So far, therefore, the T594M mutation has been identified only in individuals of African descent (*11–15*). However, our intensive sequence study clearly showed that this mutation is also present in the Japanese population, even though

Table 4. Clinical Profiles of Hypertensives with Missense Mutations in Exon12 of *SCNN1G*

	Case		
	1	2	3
Polymorphism	Ala578Val	Pro603Ser	Leu609Phe
Age (years old)	70	80	65
Sex	female	male	male
BMI (kg/m^2)	21.5	25.5	24.4
Diagnosis	EHT, NIDDM	EHT, NIDDM, HL	EHT, EA
HT duration (years)	30	32	7
HT family Hx	none	mother	none
SBP (mmHg)	134	160	128
DBP (mmHg)	74	110	90
Medication	CCB, ACEI, ARB	CCB	−
Na (mEq/l)	143	140	140
K (mEq/l)	3.8	4.2	4.3
Cl (mEq/l)	106	105	106
Creatinine (mg/dl)	0.5	1.2	1.0
Overt proteinuria	−	+	−
PRA (ng/ml/h)	0.3	1.3	2.8
PAC (ng/dl)	12.2	9.8	15.6
FBS (mg/dl)	136	105	93
HbA1c (mg/dl)	8.6	6.1	4.6

SCNN1G, γ-subunit of epithelial sodium channel gene; BMI, body mass index; EHT, essential hypertension; NIDDM, non-insulin dependent diabetes mellitus; HL, hyperlipidemia; EA, effort angina; HT, hypertension; Hx, history; SBP, systolic blood pressure; DBP, diastolic blood pressure; CCB, calcium channel blocker; ACEI, angiotensin converting enzyme inhibitor; ARB, angiotensin II receptor blockade; PRA, plasma renin activity; PAC, plasma aldosterone concentration; FBS, fasting blood sugar.

the prevalence is quite low (2/956, 0.2%). In a study on black residents in London, a gender difference was observed, with females tending to carry the M allele (*18*). Notably, two individuals having the M allele in our study were also females.

Whole-cell voltage clamp recording of lymphocytes from patients having the variant channel with the T594M mutation showed a greater response following stimulation with cAMP analog compared to wild-type lymphocytes (*11*). Furthermore, the cells isolated from the homozygote showed that phorbol 12-myristate 13-acetate had no effect on cAMP analog-induced electrophysiological responses, indicating that the T594M mutation plays an important role in regulating ENaC (*17*). These functional analyses may explain the clinical phenotype of patients with the T594M mutation. The T594M mutation contributes to the elevation of blood pressure and suggests that consideration should be given to the use of amiloride in affected individuals (*19*).

In the present study, we found a novel missense mutation, E632K, in exon13 of the *SCNN1B* gene. As shown in Table 3, a patient with this missense mutation (case 6) was diagnosed with renovascular hypertension, and showed specific abnormalities in potassium level, PRA and PAC. This patient had taken angiotensin II receptor antagonist and spironolactone, but still had marked hypokalemia. Therefore, to clarify the consequences of this mutation, functional analysis of the mutant ENaC β subunit with E632K will be needed.

In previous studies, individuals with either one of two synonymous mutations, Ser520 and Thr594, in exon 13 of the *SCNN1B* gene showed no significant differences in home or casual blood pressure values, age, body mass index, biochemical profiles of electrolytes or PRA, gender, or use of antihypertensive medication compared to individuals without mutation (*13*, *16*). In the present study, we confirmed that these two mutations did not influence body mass index, biochemical profiles, or use of antihypertensive medications. However, we were not able to evaluate these mutations with respect to blood pressure elevation, since all our subjects were hypertensives.

Three hypertensive patients with novel missense mutations in exon 12 of the *SCNN1G* gene did not have specific abnormalities in electrolytes or the renin-angiotensin aldosterone system. However, it was considered worthwhile to perform functional analysis of these missense mutations in the *SCNN1G*, because single nucleotide polymorphism in the promoter region has been associated with blood pressure regulation in Japanese (*21*).

In summary, we identified three missense mutations, including one novel mutation, E632K, in the *SCNN1B* gene and three novel missense mutations, A578V, P603S and L609F, in the *SCNN1G* gene, in Japanese patients with hy-

pertension.

It remains unclear what roles these missense mutations of the *SCNN1B* or *SCNN1G* gene play in the pathogenesis of hypertension and the regulation of electrolytes in hypertensive patients. Thus, further investigations, including functional analyses, of these mutations will be needed.

Acknowledgements

We are grateful to Dr. Mariko Banno, Ms. Yoko Tokunaga and Chiyako Imai for their excellent technical assistance.

References

1. Kosari F, Sheng S, Li J, Mak DO, Foskett JK, Kleyman TR: Subunit stoichiometry of the epithelial sodium channel. *J Biol Chem* 1998; **273**: 13469–13474.
2. Firsov D, Gautschi I, Merillat AM, Rossier BC, Schild L: The heterotetrameric architecture of the epithelial sodium channel (ENaC). *EMBO J* 1998; **17**: 344–352.
3. Canessa CM, Merillat AM, Rossier BC: Membrane topology of the epithelial sodium channel in intact cells. *Am J Physiol* 1994; **267**: 1682–1690.
4. Canessa CM, Schild L, Buell G, *et al*: Amiloride-sensitive epithelial Na^+ channel is made of three homologous subunits. *Nature* 1994; **367**: 463–467.
5. Shimkets RA, Warnock DG, Bositis CM, *et al*: Liddle's syndrome: heritable human hypertension caused by mutations in the β subunit of the epithelial sodium channel. *Cell* 1994; **79**: 407–414.
6. Hansson JH, Schild L, Lu Y, *et al*: A *de novo* missense mutation of the β subunit of the epithelial sodium channel causes hypertension and Liddle syndrome, identifying a proline-rich segment critical for regulation of channel activity. *Proc Natl Acad Sci USA* 1995; **92**: 11495–11499.
7. Hansson JH, Nelson-Williams C, Suzuki H, *et al*: Hypertension caused by a truncated epithelial sodium channel γ subunit: genetic heterogeneity of Liddle syndrome. *Nat Genet* 1995; **11**: 76–82.
8. Snyder PM, Price MP, McDonald FJ, *et al*: Mechanism by which Liddle's syndrome mutations increase activity of a human epithelial Na^+ channel. *Cell* 1995; **83**: 969–978.
9. Schild L, Lu Y, Gautschi I, Schneeberger E, Lifton RP, Rossier BC: Identification of a PY motif in the epithelial Na channel subunits as a target sequence for mutations causing channel activation found in Liddle syndrome. *EMBO J* 1996; **15**: 2381–2387.
10. Staub O, Dho S, Henry PC, *et al*: WW domains of Nedd 4 bind to the proline-rich PY motifs in the epithelial Na^+ channel deleted in Liddle's syndrome. *EMBO J* 1996; **15**: 2371–2380.
11. Su YR, Rutkowski MP, Klanke CA, *et al*: A novel variant of the β-subunit of the amiloride-sensitive sodium channel in African Americans. *J Am Soc Nephrol* 1996; **7**: 2543–2549.
12. Persu A, Barbry P, Bassilana F, *et al*: Genetic analysis of the β subunit of the epithelial Na^+ channel in essential hypertension. *Hypertension* 1998; **32**: 129–137.
13. Matsubara M, Ohkubo T, Michimata M, *et al*: Japanese individuals do not harbor the T594M mutation but do have the P592S mutation in the *C*-terminus of the β-subunit of the epithelial sodium channel: the Ohasama study. *J Hypertens* 2000; **18**: 861–866.
14. Sugiyama T, Kato N, Ishinaga Y, Yamori Y, Yazaki Y: Evaluation of selected polymorphisms of the Mendelian hypertensive disease genes in the Japanese population. *Hypertens Res* 2001; **24**: 515–521.
15. Dong YB, Zhu HD, Baker EH, *et al*: T594M and G442V polymorphisms of the sodium channel β subunit and hypertension in a black population. *J Hum Hypertens* 2001; **15**: 425–430.
16. Matsubara M, Metoki H, Suzuki M, *et al*: Genotypes of the βENaC gene have little influence on blood pressure level in the Japanese population. *Am J Hypertens* 2002; **15**: 189–192.
17. Cui Y, Su YR, Rutkowski M, Reif M, Menon AG, Pun RYK: Loss of protein kinase C inhibition in the β-T594M variant of the amiloride-sensitive Na^+ channel. *Proc Natl Acad Sci USA* 1997; **94**: 9962–9966.
18. Baker EH, Dong YB, Sagnella GA, *et al*: Association of hypertension with T594M mutation in β subunit of epithelial sodium channels in black people resident in London. *Lancet* 1998; **351**: 1388–1392.
19. Baker EH, Duggal A, Dong Y, *et al*: Amiloride, a specific drug for hypertension in black people with T594M variant? *Hypertension* 2002; **40**: 13–17.
20. Warnock DG: T594M mutation in the ENaC β subunit and low-renin hypertension in blacks. *Am J Kidney Dis* 1999; **34**: 579–583.
21. Iwai N, Baba S, Mannami T, *et al*: Association of sodium channel γ-subunit promoter variant with blood pressure. *Hypertension* 2001; **38**: 86–89.
22. Okuda T, Fujioka Y, Kamide K, *et al*: Verification of 525 coding SNPs in 179 hypertension candidate genes in the Japanese population: identification of 159 SNPs in 93 genes. *J Hum Genet* 2002; **47**: 387–394.
23. Tanaka C, Kamide K, Takiuchi S, *et al*: An alternative fast and convenient genotyping method for the screening of angiotensin converting enzyme gene polymorphisms. *Hypertens Res* 2003; **26**: 301–306.
24. Chang H, Fujita T: Lack of mutations in epithelial sodium channel β-subunit gene in human subjects with hypertension. *J Hypertens* 1996; **14**: 1417–1419.
25. Orita M, Iwahana H, Kanazawa H, Hayashi K, Sekiya T: Detection of polymorphisms of human DNA by gel electrophoresis as single-strand conformation polymorphisms. *Proc Natl Acad Sci USA* 1989; **86**: 2766–2770.

Original Article

Evaluation of the Lys198Asn and −134delA Genetic Polymorphisms of the Endothelin-1 Gene

Chihiro TANAKA, Kei KAMIDE*, Shin TAKIUCHI*, Yuhei KAWANO*, and Toshiyuki MIYATA

Endothelin-1 (ET-1) is a potent vasoconstrictor and shows various pharmacological responses. Two single nucleotide polymorphisms in the ET-1 gene (*EDN1*) have been reported to be associated with blood pressure (BP). One is the Lys198Asn polymorphism, which showed a positive association with BP in overweight people. Another is the 3A/4A polymorphism (−134delA) located in the 5′-untranslated region. In this study, we investigated the expression of the Lys198Asn polymorphism in ET-1 *in vitro*, as well as the association between either of the two polymorphisms and the plasma ET-1 level. We expressed both the major (Lys-type) and minor type (Asn-type) preproET-1 in three different cell lines, and measured the levels of ET-1 and big ET-1 in the culture supernatant. There was no significant difference in the levels of ET-1 or big ET-1 between the Asn-type and Lys-type transfectant. In the association study, the plasma levels of ET-1 in 54 hypertensive patients having an amino acid substitution from Lys to Asn at position 198 were not different from those of hypertensives without the substitution. However, we found a significant difference in ET-1 levels between individuals with the 3A/3A and 3A/4A genotypes. Our transient expression study indicates that the Lys198Asn polymorphism may not directly affect ET-1 and big ET-1 production. Another variant in the *EDN1* gene in linkage disequilibrium with the Lys198Asn polymorphism may be responsible for the association with BP, or the interaction between the *EDN1* Lys198Asn polymorphism and other factors such as obesity may be involved in the mechanisms elevating BP *in vivo*. (*Hypertens Res* 2004; 27: 367–371)

***Key Words*: endothelin-1, Lys198Asn polymorphism, hypertension, vasoactive peptide, plasma endothelin-1 level**

Introduction

Endothelin-1 (ET-1), a 21-amino-acid peptide, is a potent vasoconstrictor and pressor substance mainly produced by vascular endothelial cells (*1*). ET-1 is thought to contribute to the development of cardiovascular diseases, and is assumed to modulate vascular tone and blood flow and promote vascular cell growth in an autocrine or paracrine fashion through two subtypes of receptor (*2*). In a previous clinical study, the plasma ET-1 level was significantly higher in essential hypertensive patients (*3*). Furthermore, an elevated ET-1 level has been associated with carotid atherosclerosis and asymptomatic cerebrovascular lesions in patients with essential hypertension (*4*). Thus, it is thought that ET-1 plays an important role in the etiology of hypertension and atherosclerosis (*5*).

ET-1 is synthesized from a 212-amino-acid precursor protein, preproET-1, through multiple proteolytic steps, as shown in Fig. 1 (*2*, *6*, *7*). In the first step, preproET-1 is cleaved by signal peptidase, resulting in the formation of proET-1. ProET-1 is then cleaved at the paired dibasic amino acids by a furin-like enzyme to give rise to 38-amino-acid big ET-1 or other intermediates. Big ET-1 is subsequently cleaved at Trp73-Val74 by another endopeptidase, endothelin converting enzyme (ECE), resulting in the production of mature ET-1. Although ET-1 is biologically active, intermediate polypeptides, including big ET-1, are bio-

From the Research Institute and *Division of Hypertension and Nephrology, National Cardiovascular Center, Osaka, Japan.

This study was supported by the Program for Promotion of Fundamental Studies in Health Science of the Organization for Pharmaceutical Safety and Research of Japan.

Address for Reprints: Kei Kamide, M.D., Division of Hypertension and Nephrology, National Cardiovascular Center, 5-7-1 Fujishirodai, Suita, 565-8565, Japan. E-mail: kamide@hsp.ncvc.go.jp

Received December 8, 2003; Accepted in revised form February 4, 2004.

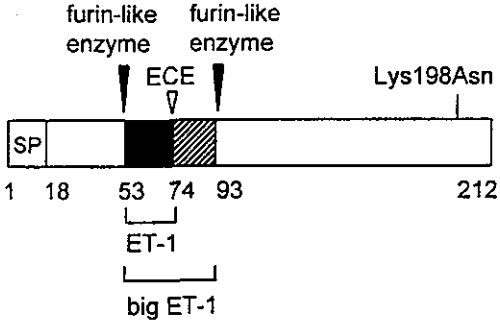

Fig. 1. *Processing of preproendothelin-1. The cleavage sites of furin-like enzyme and endothelin converting enzyme are shown by black and white arrowheads, respectively. ET-1 is a 21-amino acid peptide with residues 53–73. Big ET-1 is a 40-amino acid peptide with residues 53–92. The position of the Lys198Asn polymorphism is also shown by an arrow. SP, signal peptide; ET-1, endothelin-1; ECE, endothelin converting enzyme.*

logically inactive (*8*).

There are two single nucleotide polymorphisms in the ET-1 gene (*EDN1*) that are associated with blood pressure (BP). A G-to-T transversion in exon 5 that causes the Lys-to-Asn substitution at codon 198 has been reported (*9–11*). Recent association studies suggest that the Lys198Asn polymorphism interacts with BP in overweight people (*9, 10*), or with body mass index (BMI) in association with hypertension (*11*). Concerning plasma ET-1 level, pregnant women with the Asn/Asn genotype have significantly elevated plasma ET-1 levels, and the Asn-allele has been associated with raised systolic BP (SBP), suggesting the functional importance of this polymorphism in pregnancy (*12*). In a study using human mammary artery rings *in vitro*, artery segments from individuals with the Lys/Lys genotype were found to have an elevated response to phenylephrine-induced contractions compared to those with the Lys/Asn or Asn/Asn genotype (*13*).

Another polymorphism associated with hypertension is the 3A/4A variant (−134delA) located 138 bp downstream from the transcription start site in the 5′-untranslated region in *EDN1* (*14, 15*). In an *in vitro* assay for using the luciferase reporter gene, Popowski *et al.* reported that the 4A allele showed increased expression compared to the 3A allele (*16*). Furthermore, the human umbilical vein endothelial cells (HUVECs) obtained from homozygotes with the 4A allele showed a significantly increased expression of ET-1 protein due to enhanced mRNA stability (*16*). However, the association of plasma ET-1 levels with the 3A/4A genotypes has not been investigated.

The studies on the Lys198Asn polymorphism so far performed (*9–13*) have raised the question of whether the Lys198Asn polymorphism by itself has functional significance or, alternatively, whether it is linked to another variant in the *EDN1* gene. The Lys198Asn polymorphism is located near the carboxyl terminal region, which is removed from preproET-1 by the proteolytic action of the furin-like enzyme (Fig. 1). If the *EDN1* Lys198Asn polymorphism is directly involved in the ET-1 function, it may affect the processing of preproET-1 to mature ET-1 through big ET-1 formation. To test this hypothesis, we performed transfection experiments. We measured the concentration of ET-1 and big ET-1 in the culture supernatant obtained from Lys-type or Asn-type transfectants using three different cell lines. In addition, we measured the plasma levels of ET-1 and investigated the influence of two *EDN1* polymorphisms, Lys198Asn and 3A/4A, on the plasma ET-1 level in patients with hypertension.

Methods

Cell Culture

COS1 cells and 293 cells were purchased from American Type Culture Collection (Manassas, USA), and HUVECs were purchased from CellSystems (St. Katharinen, Germany). COS1 and 293 cells were cultured in DMEM medium (Invitrogen, Carlsbad, USA) supplemented with 10% fetal bovine serum (FBS) (JRH Biosciences, Lenexa, USA), while HUVECs were cultured on a type I collagen-coated culture dish in MCDB131 medium (Invitrogen) supplemented with 10 mmol/l GlutaMAX (Invitrogen), 20 mmol/l HEPES (Invitrogen), 2% FBS, and 10 ng/ml basic fibroblast growth factor (Roche Diagnostics, Mannheim, Germany). These cells were incubated in humidified 5% CO_2 in air at 37°C. HUVECs were used for the experiments after 3–5 passages.

Site-Directed Mutagenesis

The preproendothelin-1 cDNA covering the entire coding region was subcloned between the *Eco*RI and *Sal*I sites of the pCI mammalian expression vector (Promega, Madison, USA). Since this cDNA encodes Lys at codon 198, the obtained expression vector was designated pCI/hET-1/Lys. To replace Lys with Asn at codon 198, site-directed mutagenesis was performed. The following primers were used for polymerase chain reaction with a *Pfu* DNA polymerase (Stratagene, La Jolla, USA) (the mutated codon is underlined): forward 5′-CAAGCTGAAAGGCAATCCCTCCAGAGAGCG-3′, and reverse 5′-CGCTCTCTGGAGGGATTGCCTTTCAGCTTG-3′. Successful introduction of this mutation was confirmed by sequencing the entire coding region, and the obtained plasmid was designated pCI/hET-1/Asn.

Transient Expression and Measurement of the Concentration of Extracellular ET-1

COS1 cells were seeded at 1×10^5 cells/well in six-well plates on the day before transfection, and transfected with a mixture of 1 μg of expression plasmid (pCI/hET-1/Lys, pCI/hET-1/Asn or pCI) and 5 ng of pMI-SEAP (Roche

Diagnostics) using 5 μl of Polyfect Transfection Reagent (QIAGEN, Hilden, Germany) according to the manufacturer's instructions. After a 24-h incubation, the culture medium was exchanged to fresh medium containing 10% FBS. The transfected cells were incubated for another 24 h and then the culture supernatant was collected for measurement of immunoreactive ET-1 and big ET-1. The activity of secreted human placental alkaline phosphatase (SEAP) in the culture supernatant was measured by SEAP Reporter Gene Assay (Roche Diagnostics) for normalization of the transfection efficiency. The 293 cells were seeded at 2×10^5cells/well in six-well plates and transfected by the same method as used for the COS1 cells, except for the use of 3 μl of FuGENE 6 Transfection Reagent (Roche Diagnostics). HUVECs were seeded at 1×10^5cells/well in six-well plates and transfected with a mixture of 0.5 μg of expression plasmid and 5 ng of pMI-SEAP using 3 μl of FuGENE 6 Transfection Reagent. After a 6-h incubation, the culture medium was exchanged with fresh medium. The transfected cells were incubated for another 42 h, and then the culture supernatant was collected. The amounts of immunoreactive ET-1 and big ET-1 in the culture supernatant were measured by enzyme-linked immunosorbent assay (ELISA) using the Endothelin-1 Measurement Kit-IBL and Human Big Endothelin-1 Measurement Kit-IBL, respectively (Immuno-Biological Laboratories Co., Ltd., Fujioka, Japan).

Comparison of the Plasma ET-1 Level between Each Genotype in *EDN1* Gene Polymorphisms

We measured the plasma ET-1 level and genotyped two *EDN1* gene polymorphisms, Lys198Asn (5727G>T) in exon 5 and 3A/4A in the 5′-untranslated region (−134delA), in 54 randomly selected essential hypertensive patients enrolled at the Division of Hypertension and Nephrology at the National Cardiovascular Center. All subjects provided written informed consent to participate in the study, and the study protocol was approved by the Ethical Review Committee of the National Cardiovascular Center. The plasma ET-1 level was measured by radioimmunoassay after extraction (*17*). Genotyping was performed by the TaqMan PCR method using the following probes and primers: for Lys198Asn, probes Fam-AGGCAAGCCCTCCA-MGB (Lys-allele), Vic-AAGG CAATCCCTCCAG-MGB (Asn-allele), and primers 5′-CAG CGTCAAATCATCTTTTCATG-3′ and 5′-GTCACCAATG TGCTCGGTTGT-3′, and for 3A/4A, probes Fam-AGTGCC CTTTTAACGG-MGB (4A-allele) and Vic-AAGTGCCC TTTAACGG-MGB (3A-allele), and primers 5′-AAACAGC TTCAGGTCCCTCAAA-3′ and 5′-GCAGTCCCAGCTCTC CACC-3′ (*18*).

Statistical Analysis

The comparison of ET-1 and big ET-1 levels in the culture supernatant between the different transfected cell lines, and of the plasma ET-1 level and all of the clinical parameters between the two genotypes in patients with essential hypertension were performed by unpaired Student's *t*-test using the program StatView (SAS Institute, Inc., Cary, USA). A value of $p<0.05$ was considered to be statistically significant. In order to evaluate the linkage disequilibrium (LD), we calculated the D' and r^2 value using SNPAlyze version 3.0 software (DYNACOM, Mobara, Japan).

Results

The Lys198Asn Polymorphism Did Not Affect the ET-1 and Big ET-1 Levels in the Culture Supernatant

To examine whether the Lys198Asn polymorphism in the *EDN1* gene affects production of ET-1, *COS1* cells were transfected with either a Lys-type plasmid or Asn-type plasmid, and the amounts of secreted ET-1 were measured by ELISA. Since ECE is expressed in many cell lines, including COS1 cells, preproET-1 should be converted to ET-1. In the culture supernatant collected from the cells transfected with either the Lys-type or Asn-type plasmid, higher levels of ET-1 were detected as compared with that in cells transfected with the vector alone (Fig. 2A, left panel). No difference in ET-1 level was observed between the Lys-type and Asn-type transfected cells (Fig 2A, left panel). We also measured the big ET-1 levels. The amount of big ET-1 in the supernatant was much higher than that of ET-1, and also was not significantly different between Asn-type and Lys-type transfected cells (Fig. 2A, right panel). Using co-transfected pMI-SEAP plasmid, we normalized the transfection efficiency of the plasmids, but the results were same.

Regarding the other cell lines, 293 cells and HUVECs, there were no significant differences in either the ET-1 or big ET-1 levels in the culture supernatant between Asn-type and Lys-type transfected cells, as indicated in COS1 cells (Fig. 2B, C). Normalization of the transfection efficiency by co-transfection of pMI-SEAP plasmid did not alter the results.

Relationship between *EDN1* Gene Polymorphism and Plasma ET-1 Level in Hypertensives

We assessed the difference in plasma ET-1 level between genotypes in Lys198Asn (5727G>T) and 3A/4A (−134delA) in 54 patients with essential hypertension (mean age: 61.0± 12.8 years old; male/female: 30/24; mean BMI: 25.3± 3.6 kg/m^2; mean BP: 144.5±17.3/82.2±10.5 mmHg). As shown in Fig. 3A, the plasma levels of ET-1 tended to be higher in subjects with the Asn-allele (GT+TT) than in homozygotes with 198Lys (GG), but the difference was not significant ($p=0.057$). In contrast, there was a significant difference in plasma ET-1 level between 3A/3A and 3A/4A (Fig. 3B). There were no differences in age, sex, BMI, BP levels or renal function between the two genotypes of these *EDN1* gene polymorphisms (data not shown).

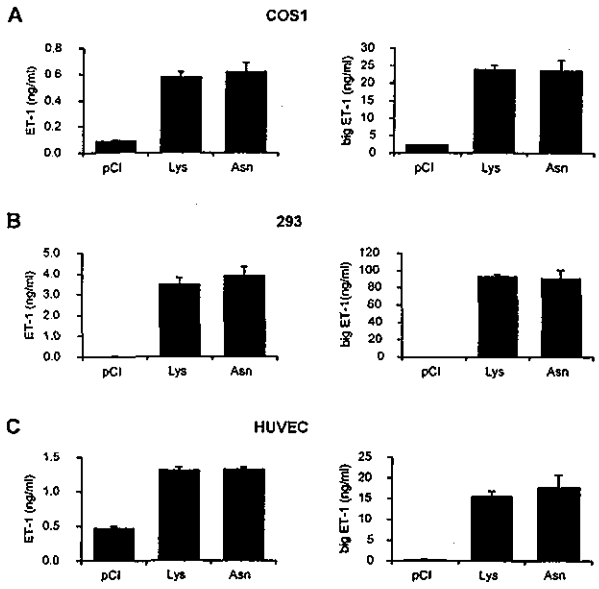

Fig. 2. *A: Levels of ET-1 (left panel) and big ET-1 (right panel) in the culture supernatant of COS1 cells. B: Levels of ET-1 (left panel) and big ET-1 (right panel) in the culture supernatant of 293 cells. C: Levels of ET-1 (left panel) and big ET-1 (right panel) in the culture supernatant of HUVECs. Each cell line was transfected with pCI/hET-1/Lys, pCI/hET-1/Asn or pCI. The levels of ET-1 and big ET-1 in the culture supernatant were measured by ELISA. The data represent the means±SD from three independent experiments. ET-1, endothelin-1; HUVECs, human umbilical vein endothelial cells.*

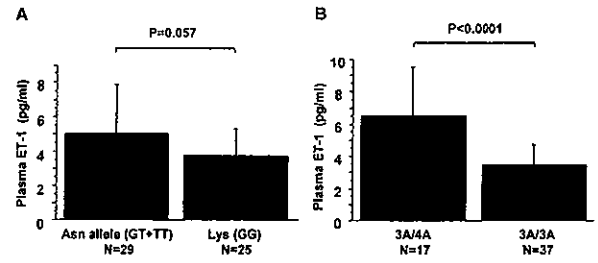

Fig. 3. *A: Comparison of plasma ET-1 level between Asn-allele and Lys homozygotes of the* EDN1 *Lys198Asn polymorphism (5727G>T). B: Comparison of plasma ET-1 level between 3A/3A and 3A/4A of the* EDN1 *3A/4A polymorphism in the 5′-untranslated region (−134delA). The data represent the means±SD. ET-1, endothelin-1.*

Discussion

Several reports have described that the Lys198Asn polymorphism in preproET-1 showed a positive association with BP elevation in overweight people, and this was observed not only in Caucasians but also in Japanese (*9–11*). Another study focusing on pregnant women showed that the Asn-allele was associated with SBP, and homozygotes with Asn198 had a significantly increased level of plasma ET-1 compared to women with other genotypes (*12*). These studies suggested that the Lys198Asn polymorphism may affect BP regulation through the production of ET-1. However, none of the studies examined the functional consequence of the Lys198Asn polymorphism on preproET-1. Because the Lys198Asn polymorphism is located in the coding region of the *EDN1* gene, it is likely that the polymorphism affects the processing of preproET-1 rather than modifying the gene expression or the stability of the mRNA. Here, we have designed a strategy to test this hypothesis by expressing the Lys-type and Asn-type preproET-1 transiently in three different cell lines, COS1 cells, 293 cells and HUVECs. The results showed that neither ET-1 nor big ET-1 levels in the culture supernatant of the Asn-type transfected cells were significantly changed compared to those of the Lys-type transfected cells.

The amount of big ET-1 in the medium was much higher than that of ET-1 in all cell types (Fig. 2). ET-1 is synthesized from big ET-1 through proteolytic cleavage by ECE. The large amount of big ET-1 in the culture supernatant indicated the inefficient cleavage of big ET-1 by endogenous ECE, because transient expression of preproET-1 using cytomegalovirus promoter would result in overproduction of big ET-1 for the endogenous enzyme.

It has been reported that ET-1[1–31], a peptide 10 amino acids longer than ET-1, is synthesized from big ET-1 by the proteolytic action of chymase and is also bioactive (*19–21*). The Lys198Asn polymorphism might affect the production of ET-1[1–31]. Unfortunately, in the present study, ET-1[1–31] could not be detected in the culture supernatant by ELISA (data not shown), probably due to the very low activity of chymase in the cells that we used.

In the measurement of the plasma ET-1 level in the 54 patients with essential hypertension, we were not able to find a significant difference between the genotypes in the *EDN1* Lys198Asn polymorphism, though the Asn-allele subjects tended to have a higher plasma ET-1 level than subjects with the Lys-allele. This finding seems to be concordant with the results obtained from the transfection study. Barden *et al.*, however, reported that plasma ET-1 levels were increased in Asn homozygotes in pregnant women (*12*). In addition, the positive correlation between this polymorphism and high BP has been observed only in overweight subjects (*9*, *10*). Thus, it is suggested that a study focusing on normotensives is necessary, because the expression and/or production of ET-1 might be modified by BP or other factors such as obesity. Furthermore, the interaction between the *EDN1* Lys198Asn polymorphism and other factors, such as insulin resistance or activation of the renin-angiotensin system, may be involved in the mechanisms elevating BP *in vivo*.

An association between hypertension and the 3A/4A polymorphism (−134delA) located 138 bp downstream from the transcription start site in the 5′-untranslated region in the

EDN1 gene has been reported (*14*, *15*). Popowski *et al.* reported that the HUVECs obtained from homozygotes with the 4A-allele type showed a significantly increased expression of ET-1 protein due to enhanced mRNA stability (*16*). In the present study, significantly higher plasma ET-1 levels were observed in hypertensive subjects with the 4A-allele compared to 3A/3A homozygotes, although Popowski *et al.* could not find increased expression of ET-1 in the HUVECs obtained from heterozygotes. The reason why they did not observe the increased secretion of ET-1 in the *ex vivo* system was likely due to the difference in the background of the individuals—that is, they obtained their results using HUVECs from healthy German newborns and our results were obtained from Japanese hypertensives. LD analysis revealed that the Lys198Asn and 3A/4A polymorphisms are slightly in LD ($D'=0.65$, $r^2=0.20$). In the present study, the tendency for a positive correlation between the Lys198Asn polymorphism and plasma ET-1 levels was also recognized.

In conclusion, our results indicated that the *EDN1* Lys198Asn polymorphism did not directly affect ET-1 production in the expression assay using cultured transfected cells. Therefore, we propose that another variant having LD with this polymorphism, such as maybe the 3A/4A polymorphism, might be responsible for the association with BP elevation *via* plasma ET-1 up-regulation, or the interaction between the *EDN1* Lys198Asn polymorphism and other factors such as obesity might be involved in the mechanisms elevating BP *in vivo*.

Acknowledgements

We thank Dr. T. Sawamura at the Research Institute of the National Cardiovascular Center for providing human preproET-1 cDNA.

References

1. Yanagisawa M, Kurihara H, Kimura S, *et al*: A novel potent vasoconstrictor peptide produced by vascular endothelial cells. *Nature* 1988; **332**: 411–415.
2. Miyauchi T, Masaki T: Pathophysiology of endothelin in the cardiovascular system. *Annu Rev Physiol* 1999; **61**: 391–415.
3. Kohno M, Yasunari K, Murakawa K, *et al*: Plasma immunoreactive endothelin in essential hypertension. *Am J Med* 1990; **88**: 614–618.
4. Minami S, Yamano S, Yamamoto Y, *et al*: Associations of plasma endothelin concentration with carotid atherosclerosis and asymptomatic cerebrovascular lesions in patients with essential hypertension. *Hypertens Res* 2001; **24**: 663–670.
5. Schiffrin EL: Role of endothelin-1 in hypertension and vascular disease. *Am J Hypertens* 2001; **14**: 83S–89S.
6. Kido T, Sawamura T, Hoshikawa H, *et al*: Processing of proendothelin-1 at the C-terminus of big endothelin-1 is essential for proteolysis by endothelin-converting enzyme-1 *in vivo*. *Eur J Biochem* 1997; **244**: 520–526.
7. Kido T, Sawamura T, Masaki T: The processing pathway of endothelin-1 production. *J Cardiovasc Pharmacol* 1998; **31** (Suppl 1): S13–S15.
8. Kimura S, Kasuya Y, Sawamura T, *et al*: Conversion of big endothelin-1 to 21-residue endothelin-1 is essential for expression of full vasoconstrictor activity: structure-activity relationships of big endothelin-1. *J Cardiovasc Pharmacol* 1989; **13** (Suppl 5): S5–S7.
9. Tiret L, Poirier O, Hallet V, *et al*: The Lys198Asn polymorphism in the endothelin-1 gene is associated with blood pressure in overweight people. *Hypertension* 1999; **33**: 1169–1174.
10. Asai T, Ohkubo T, Katsuya T, *et al*: Endothelin-1 gene variant associates with blood pressure *in* obese Japanese subjects: the Ohasama Study. *Hypertension* 2001; **38**: 1321–1324.
11. Jin JJ, Nakura J, Wu Z, *et al*: Association of endothelin-1 gene variant with hypertension. *Hypertension* 2003; **41**: 163–167.
12. Barden AE, Herbison CE, Beilin LJ, Michael CA, Walters BN, Van Bockxmeer FM: Association between the endothelin-1 gene Lys198Asn polymorphism blood pressure and plasma endothelin-1 levels in normal and pre-eclamptic pregnancy. *J Hypertens* 2001; **19**: 1775–1782.
13. Iglarz M, Benessiano J, Philip I, *et al*: Preproendothelin-1 gene polymorphism is related to a change in vascular reactivity in the human mammary artery *in vitro*. *Hypertension* 2002; **39**: 209–213.
14. Stevens PA, Brown MJ: Genetic variability of the ET-1 and the ETA receptor genes in essential hypertension. *J Cardiovasc Pharmacol* 1995; **26** (Suppl 3): S9–S12.
15. Lajemi M, Gautier S, Poirier O, *et al*: Endothelin gene variants and aortic and cardiac structure in never-treated hypertensives. *Am J Hypertens* 2001; **14**: 755–760.
16. Popowski K, Sperker B, Kroemer HK, *et al*: Functional significance of a hereditary adenine insertion variant in the 5′-UTR of the endothelin-1 gene. *Pharmacogenetics* 2003; **13**: 445–451.
17. Barden A, Beilin LJ, Ritchie J, Walters BN, Michael CA: Plasma and urinary endothelin 1, prostacyclin metabolites and platelet consumption in pre-eclampsia and essential hypertensive pregnancy. *Blood Press* 1994; **3**: 38–46.
18. Tanaka C, Kamide K, Takiuchi S, *et al*: An alternative fast and convenient genotyping method for the screening of angiotensin converting enzyme gene polymorphisms. *Hypertens Res* 2003; **26**: 301–306.
19. Nakano A, Kishi F, Minami K, Wakabayashi H, Nakaya Y, Kido H: Selective conversion of big endothelins to tracheal smooth muscle-constricting 31-amino acid-length endothelins by chymase from human mast cells. *J Immunol* 1997; **159**: 1987–1992.
20. Yoshizumi M, Inui D, Okishima N, *et al*: Endothelin-1-(1–31), a novel vasoactive peptide, increases $[Ca^{2+}]_i$ in human coronary artery smooth muscle cells. *Eur J Pharmacol* 1998; **348**: 305–309.
21. Yoshizumi M, Kagami S, Suzaki Y, *et al*: Effect of endothelin-1(1–31) on human mesangial cell proliferation. *Jpn J Pharmacol* 2000; **84**: 146–155.

THE JOURNAL OF BIOLOGICAL CHEMISTRY
Vol. 279, No. 29, Issue of July 16, pp. 30896–30903, 2004
Printed in U.S.A.

Identification of Strain-specific Variants of Mouse *Adamts13* Gene Encoding von Willebrand Factor-cleaving Protease*

Received for publication, December 26, 2003, and in revised form, May 7, 2004
Published, JBC Papers in Press, May 10, 2004, DOI 10.1074/jbc.M314184200

Fumiaki Banno‡, Kazuyoshi Kaminaka§, Kenji Soejima§, Koichi Kokame‡, and Toshiyuki Miyata‡¶

From the ‡National Cardiovascular Center Research Institute, Osaka 565-8565, Japan and the §First Research Department, The Chemo-Sero-Therapeutic Research Institute, Kumamoto 869-1298, Japan

Human *ADAMTS13* was recently identified as a gene encoding von Willebrand factor-cleaving protease, hADAMTS13. Both congenital and acquired defects in this enzyme can cause thrombotic thrombocytopenic purpura. hADAMTS13 consists of 1,427 amino acid residues and is composed of multiple structural domains including thrombospondin type 1 motifs and CUB domains. To analyze the functional roles of these domains *in vivo*, we determined the cDNA sequence of the mouse ortholog, mADAMTS13. Unexpectedly, two forms of the mouse *Adamts13* gene were isolated that differed in the insertion of an intracisternal A particle (IAP) retrotransposon including a premature stop codon. The IAP insertion was found in BALB/c, C3H/He, C57BL/6, and DBA/2 strains but not in the 129/Sv strain. The outbred ICR strain had either the IAP-free or IAP-inserted allele or both. IAP-free *Adamts13* encoded mADAMTS13L, a protein of 1,426 amino acid residues with the same domain organization as hADAMTS13. In contrast, IAP-inserted *Adamts13* encoded a C-terminally truncated enzyme, mADAMTS13S, that is comprised of only 1,037 amino acid residues and lacking the C-terminal two thrombospondin type 1 motifs and two CUB domains. Strain specificity was also confirmed by reverse transcription-PCR and Northern blot analyses. Both recombinant mADAMTS13L and mADAMTS13S exhibited von Willebrand factor cleaving activities *in vitro*. The natural variation in mouse ADAMTS13 should allow for the determination of hitherto unknown functions of its C-terminal domains *in vivo*.

von Willebrand factor (VWF)[1] is a large glycoprotein that mediates adhesion between the platelet surface and damaged subendothelium (1, 2). VWF is mainly synthesized in endothelial cells and secreted into the circulating blood as unusually large VWF (UL-VWF) multimers (1, 2). In healthy individuals, UL-VWF multimers are cleaved to smaller sizes in plasma (3). If cleavage is impaired, however, UL-VWF multimers accumulate in the plasma. Because UL-VWF multimers possess an extremely high thrombotic activity (4, 5), UL-VWF multimers in the circulation lead to platelet clumping at the sites of vascular injury. The importance of VWF proteolysis is best illustrated by the severe consequences of thrombotic thrombocytopenic purpura, a condition associated with increased levels of UL-VWF multimers (6). This disease is characterized by microangiopathic hemolytic anemia, thrombocytopenia, neurological dysfunction, renal failure, and fever (7). The mortality of affected patients may exceed 90% without treatment such as plasma exchange.

Human ADAMTS13 (hADAMTS13), an enzyme responsible for the proteolytic processing of UL-VWF multimers, was recently purified, and its partial amino acid sequence was determined (8–10). hADAMTS13 cleaves a peptidyl bond between Tyr^{1605} and Met^{1606} in the VWF A2 domain (11–13). The gene encoding hADAMTS13 was identified as a member of the "a disintegrin-like and metalloprotease with thrombospondin type 1 motif (ADAMTS)" family and designated as *ADAMTS13* (8, 14, 15). *ADAMTS13* contains 29 exons and spans ~37 kb on chromosome 9q34 (8, 14, 15). The mRNA is detected primarily in liver (8, 14, 15). Analysis of genomic DNA in patients with congenital thrombotic thrombocytopenic purpura revealed that mutations of *ADAMTS13* could lead to an inactive enzyme (15–20). Notably, a common single nucleotide polymorphism, P475S, with ~10% heterozygosity in the Japanese population, resulted in a decrease of enzymatic activity (16).

hADAMTS13 consists of several different domains: a signal peptide, a propeptide, a reprolysin-like metalloprotease domain, a disintegrin-like domain, a thrombospondin type 1 (TSP1) motif, a cysteine-rich domain, a spacer domain, seven additional TSP1 repeats, and two CUB domains. *In vitro* studies using C-terminally truncated hADAMTS13 constructs revealed that the C-terminal TSP1 motifs and CUB domains were dispensable to maintain the VWF cleaving activity (21, 22). However, the biochemical and physiological roles of these domains *in vivo* remain to be resolved. As a first step to develop suitable animal models for following potential roles of this enzyme *in vivo*, we have cloned the mouse ortholog of hADAMTS13, mADAMTS13, and determined its complete genomic structure. In the present study, we report two types of the *Adamts13* gene in mice caused by the strain-specific insertion of an intracisternal A-particle (IAP) retrotransposon. We further examine the VWF cleaving activity of mADAMTS13.

* This work was supported in part by grants-in-aid from the Ministry of Health, Labor, and Welfare of Japan; from the Ministry of Education, Culture, Sports, Science, and Technology of Japan; from the Japan Society for the Promotion of Science; and from the Program for Promotion of Fundamental Studies in Health Sciences of the Organization for Pharmaceutical Safety and Research of Japan. The costs of publication of this article were defrayed in part by the payment of page charges. This article must therefore be hereby marked "*advertisement*" in accordance with 18 U.S.C. Section 1734 solely to indicate this fact.

The nucleotide sequence(s) reported in this paper has been submitted to the DDBJ/GenBank™/EBI Data Bank with accession number(s) AB071302, AB095445, and AB112362.

¶ To whom correspondence should be addressed: National Cardiovascular Center Research Institute, 5-7-1 Fujishirodai, Suita, Osaka 565-8565, Japan. Tel.: 81-6-6833-5012; Fax: 81-6-6835-1176; E-mail: miyata@ri.ncvc.go.jp.

[1] The abbreviations used are: VWF, von Willebrand factor; TSP1, thrombospondin type 1; UL-VWF, unusually large VWF; IAP, intracisternal A-particle; GST, glutathione *S*-transferase; RACE, rapid amplification of cDNA ends; RT, reverse transcription; ORF, open reading frame; h, human; m, mouse; HRP, horseradish peroxidase.

EXPERIMENTAL PROCEDURES

Animals—Male 129/Sv mice were purchased from Clea Japan, Inc. Male BALB/c, C3H/He, C57BL/6, DBA/2, and ICR mice were purchased from Japan SLC, Inc. Blood (~100 μl) was collected by cardiac puncture into a syringe containing 10 μl of 3.8% sodium citrate and centrifuged to obtain plasma. Spleen and liver were excised, rinsed in phosphate-buffered saline, and immediately used for DNA and RNA preparation.

DNA Sequencing—All of the sequence analyses were performed by 373A or 3700 automated DNA sequencer (Applied Biosystems) with a BigDye Terminator Kit (Applied Biosystems).

Determination of the mADAMTS13 cDNA Sequence—Total RNA was prepared from the livers of C57BL/6 and 129/Sv mice with Isogen (Nippon Gene), and poly(A)$^+$ RNA was purified with an mRNA purification kit (Amersham Biosciences) according to the manufacturer's instruction. The cDNA was synthesized from the poly(A)$^+$ RNA with a first strand cDNA synthesis kit (Amersham Biosciences). PCR was carried out with primers designed from the genomic DNA sequence (forward sequence in 5′-untranslated region, 5′-AGGAAGCTCCCAAGAGTAAACACTGCCT-3′; reverse sequence within the metalloprotease domain, 5′-TCAGAGAGGGTGATTAGCTTCACCAGGT-3′). PCR products were cloned into pCR2.1 vector using a TA Cloning™ kit (Invitrogen) and sequenced.

In addition, 3′-RACE was performed using a 3′-Full RACE Core Set (Takara), according to the manufacturer's instructions. After reverse transcription from liver poly(A)$^+$ RNA, PCR was performed using the Adaptor Primer provided with the kit and a gene-specific forward primer within the metalloprotease domain, 5′-TGGAGTTGCCTGATGGCAACCAGCA-3′. The second PCR was performed using the first PCR products as a template with Adaptor Primer and a gene-specific internal forward primer, 5′-CATCACCTTTTCCTACTTTCAACTGAAGCAG-3′. The cycling parameters were as follows: 35 cycles of 94 °C for 30 s, 55 °C for 30 s, and 72 °C for 3 min, followed by 72 °C for 7 min. PCR products were cloned into pCR2.1 vector and sequenced.

PCR Analysis of IAP Insertion in the Adamts13 Gene—Genomic DNA was extracted from ear punches of 129/Sv, BALB/c, C3H/He, C57BL/6, DBA/2, and ICR mice by DNeasy Tissue Kit (Qiagen). Presence or absence of an IAP insertion in the *Adamts13* gene was determined by PCR with HotStarTaq DNA polymerase (Qiagen). The amplification was carried out using mixture of three primers; the intron 23-specific forward primer, 5′-ACCTCTCAAGTGTTTGGGATGCTA-3′, the IAP-specific reverse primer, 5′-TCAGCGCCATCTTGTGACGGCGAA-3′, and the primer downstream of the IAP target site, 5′-TGCCAGATGGCCATGATTAACTCT-3′. PCR products were directly sequenced.

Southern Blot Analysis—Genomic DNA prepared from spleens was digested with EcoRV, separated on 0.7% agarose gel, and transferred to a nylon membrane by standard capillary blotting techniques. A genomic fragment (842 bp) upstream of the IAP target site was produced by PCR with the primers 5′-TAGGCAGCCATGGATCTGTATTAG-3′ and 5′-TGTCTGCTCTTCCAGAAATCCTTA-3′ and labeled with fluorescein-11-dUTP using Gene Images random prime labeling module (Amersham Biosciences). The blot was hybridized with the probe, and the hybridized probe was detected using the Antifluorescein-AP conjugate and the CDP-*Star* detection reagent (Amersham Biosciences) according to the manufacturer's instructions. Chemiluminescence was measured by an LAS-1000plus image analyzer (Fujifilm).

Determination of the Adamts13 Genomic Sequence—A λ phage library constructed from Sau3AI-digested genomic DNA of the 129/Sv strain was screened by a PCR-based method as described previously (23). Three independent positive phages were obtained. Each phage insert DNA was subcloned into pBluescript II SK(+) vector (Stratagene) and sequenced using the GPS-1 Genome Priming System (New England Biolabs) according to the manufacturer's instructions. The sequence data were assembled and analyzed using the Sequencher software (Gene Codes). Sequence gaps of each target DNA were filled by primer walking sequencing.

Reverse Transcription-PCR—Total RNA was extracted from the livers of six mouse strains with Isogen (Nippon Gene), and poly(A)$^+$ RNA was purified using PolyATtract mRNA Isolation Systems (Promega) and subjected to one-step RT-PCR (Qiagen). The exon 21/22-specific sense primer (5′-TTGTGGGAGAGGTCTGAAGGAACT-3′), the pseudo-exon 24-specific antisense primer (5′-TCAGCGCCATCTTGTGACGGCGAA-3′), and the exon 24/25-specific antisense primer (5′-ACAGGAGACAGAGCACTCTGTCCA-3′) were simultaneously used for the amplification. The PCR products were excised from the agarose gel and sequenced.

Northern Blot Analysis—The specific fluorescein-labeled probe (1.3 kb) was synthesized by PCR from mouse *Adamts13* cDNA as described previously (23). The primers used were a sense primer located in exon 3 (5′-ATTCTGCACCTGGAACTCCTGGTA-3′) and an antisense primer located in exon 13 (5′-CGGCTGACAATGAAGCTTTCTCCA-3′). Poly(A)$^+$ RNA (10 μg) from mouse livers were separated on 1% agarose gel containing 2% formaldehyde and transferred to a nylon membrane. Hybridization and detection using the Antifluorescein-AP conjugate and the CDP-*Star* detection reagent (Amersham Biosciences) were performed according to the manufacturer's instructions. Commercially available premade Northern blot membranes containing poly(A)$^+$ RNA from the BALB/c strain (Multiple Tissue Northern blot; Clontech) and the Swiss Webster strain (FirstChoice Northern blot; Ambion) were also analyzed using the Antifluorescein-HRP conjugate and the DNA Thunder Chemiluminescence Reagent Plus (PerkinElmer Life Sciences). Chemiluminescence was measured by an LAS-1000plus image analyzer (Fujifilm).

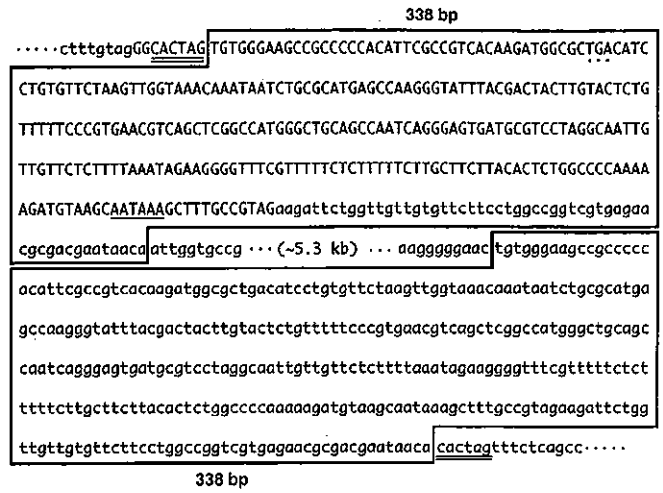

FIG. 1. **Nucleotide sequence of the retrovirus-like element observed in *Adamts13* intron 23 of the C57BL/6 strain.** The 338-bp repetitive sequences of a retrovirus-like element are *boxed*. The 6-bp duplication of target DNA at the insertion site is *double underlined*. Exon 24 of the C57BL/6 strain, shown in *uppercase letters*, contains a stop codon TGA (*dotted*) and a putative polyadenylation signal AATAAA (*underlined*).

Preparation of Recombinant Substrate (mVWF73) for Enzymatic Assay—To examine the enzymatic activities of mADAMTS13, we prepared the recombinant substrate as described previously (24). In brief, a D1596-T1668 region of mouse VWF was amplified by RT-PCR using total RNA from a C57BL/6 mouse liver. The primers, 5′-cgggatccGACCGGGTAGAGGCACCTAACC-3′ and 5′-cggaattcTCAGTGATGGTGATGGTGATGTGTCTGCAGGACCAGGTCAGGA-3′ were used for the amplification. Lowercase letters indicate added restriction enzyme *sites*, and the underlined sequence is the inserted C-terminal His_6 tag (H). The PCR product was digested with BamHI and EcoRI and cloned into the corresponding sites of pGEX-6P-1 (Amersham Biosciences), a glutathione S-transferase (GST) fusion expression vector. The resulting plasmid encoding GST-D1596T1668-H was introduced into *Escherichia coli*, BL21 (Stratagene), and expression was induced by the addition of isopropyl-β-D-thiogalactoside. The bacterial cells were collected and lysed with CelLytic B (Sigma), followed by centrifugation. The soluble fraction was subjected to a nickel-nitrilotriacetic acid Spin Kit (Qiagen) and further to a MicroSpin GST purification module (Amersham Biosciences). The purified protein, designated GST-mVWF73-H, was used as substrates for enzymatic assays. The molecular mass of GST-mVWF73-H was 35.7 kDa. If mADAMTS13 cleaves the expected site, the size of the N-terminal portion including the GST tag will be 28.0 kDa.

Transient Expression of mADAMTS13—The entire open reading frame (ORF) constructs with C-terminal FLAG sequence (DYKDDDDK) were prepared for two types of mouse ADAMTS13, mADAMTS13L (GenBank™ accession number AB112362) and mADAMTS13S (GenBank™ accession number AB071302), by PCR. Each PCR product was inserted into pCAGG-neo mammalian expression vector (25). The resulting plasmids were transfected into HeLa cells using FuGENE 6 (Roche Applied Science) as described previously (16). Forty-eight hours after transfection, the media were collected and concentrated using Centricon YM-30 (Millipore). The cells together with extracellular matrix were lysed in SDS sample buffer (10 mM

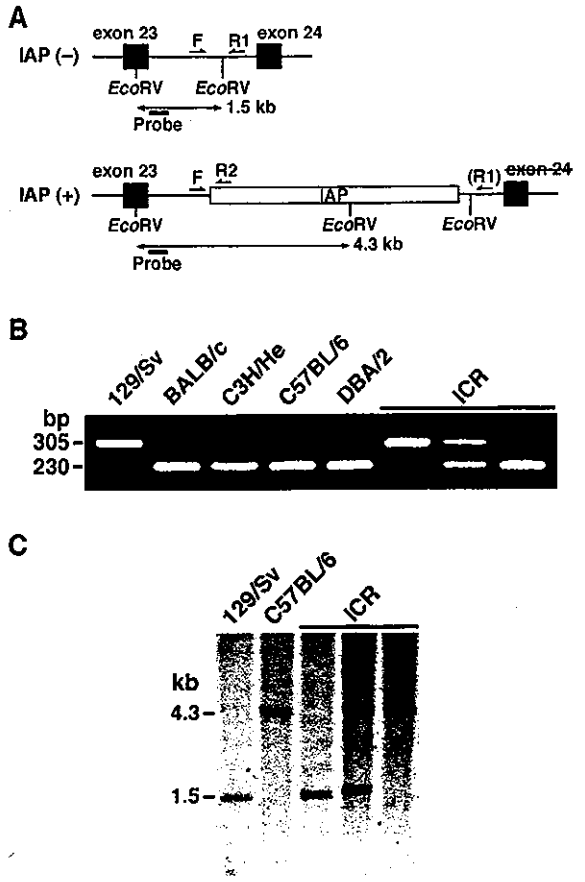

FIG. 2. **Genotyping of mouse *Adamts13*.** *A*, diagram of a segment of the *Adamts13* gene around the IAP insertion site. The sites of primers used for the genotyping PCR are indicated by *arrows*. The EcoRV fragments detected in Southern blot analysis are indicated by *double-headed arrows*. *B*, PCR analysis. In mixture of three primers, F and R1 primers generate a 305-bp product specific for the IAP-free *Adamts13* gene, whereas F and R2 primers generate a 230-bp product specific for the IAP-inserted *Adamts13* gene. *C*, Southern blot analysis. Genomic DNA from each mouse strain was digested with EcoRV and hybridized with the probe that detects a 1.5-kb fragment in the IAP-free allele and a 4.3-kb fragment in the IAP-inserted allele.

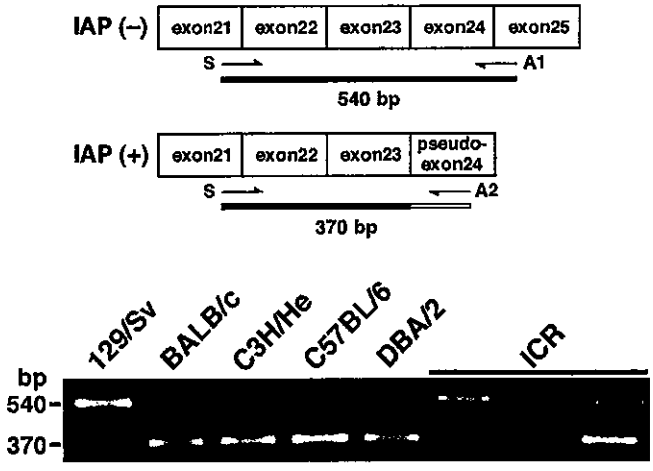

FIG. 3. **RT-PCR of *Adamts13* mRNA in liver.** PCR primers are shown as *arrows* indicating direction at their approximate locations. In combination of three primers, S and A1 primers generate a 540-bp product specific to the IAP-free transcript, whereas primers S and A2 generate a 370-bp product specific to the IAP-inserted transcript.

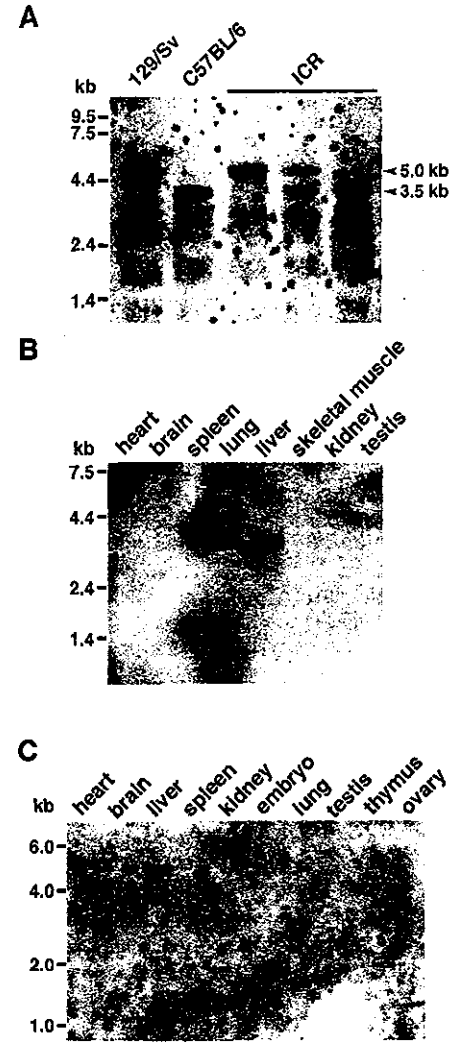

FIG. 4. **Northern blot analysis of mouse *Adamts13* mRNA.** *A*, expression of *Adamts13* mRNA in liver. Poly(A)$^+$ RNA isolated from liver of indicated strains was probed with a 1.3-kb *Adamts13* cDNA corresponding to exons 3–13. The approximate sizes of the IAP-free (5.0 kb) and the IAP chimeric (3.5 kb) transcripts are indicated by *arrowheads*. *B*, expression of *Adamts13* mRNA in tissues from BALB/c mice. *C*, expression of *Adamts13* mRNA in tissues from SwissWebster mice. The sizes of RNA markers are shown at the *left*.

Tris-HCl, 2% SDS, 50 mM dithiothreitol, 2 mM EDTA, 0.02% bromphenol blue, 6% glycerol, pH 6.8).

Recombinant proteins were detected by SDS-PAGE and Western blot as described previously (16). For culture media, a rabbit anti-mADAMTS13 polyclonal antibody (described below) and an HRP-labeled goat anti-rabbit IgG antibody (Kirkegaard & Perry Laboratories) were used for detection after SDS-PAGE under nonreducing condition. For cell lysates, an anti-FLAG M2 monoclonal antibody (Sigma) and an HRP-labeled goat anti-mouse IgG antibody (Kirkegaard & Perry Laboratories) were used for detection after SDS-PAGE under reducing condition. Chemiluminescence was developed using the Western Lighting Chemiluminescence Reagent Plus (PerkinElmer Life Sciences) and detected by an LAS-1000plus image analyzer (Fujifilm).

Preparation of Polyclonal Antibody against Mouse ADAMTS13—A polyclonal antiserum against mADAMTS13 was raised by DNA-based immunization protocols. Rabbits were immunized by intradermal injection with ~1 mg of mADAMTS13S expression plasmid at 25 sites on the back. Booster immunizations were carried out by the same protocol 3 weeks after the primary immunization. Serum was collected 3 weeks after the second immunization. The IgG fraction was then prepared by an affinity chromatography using a protein G column (Amersham Biosciences).

Enzymatic Assay—Purified GST-mVWF73-H (500 ng) was incubated with recombinant mADAMTS13L or mADAMTS13S in 40 μl of reaction buffer (5 mM Tris-HCl, 10 mM $BaCl_2$, 0.01% Tween 20, and 1 mM *p*-amidinophenylmethanesulfonyl fluoride hydrochloride, pH 8.0) at 37 °C for 1 h. The reaction was stopped by adding 10 μl of SDS sample buffer (50 mM Tris-HCl, 10% SDS, 250 mM dithiothreitol, 10 mM EDTA, 0.1% bromphenol blue, 30% glycerol, pH 6.8). The samples were sub-

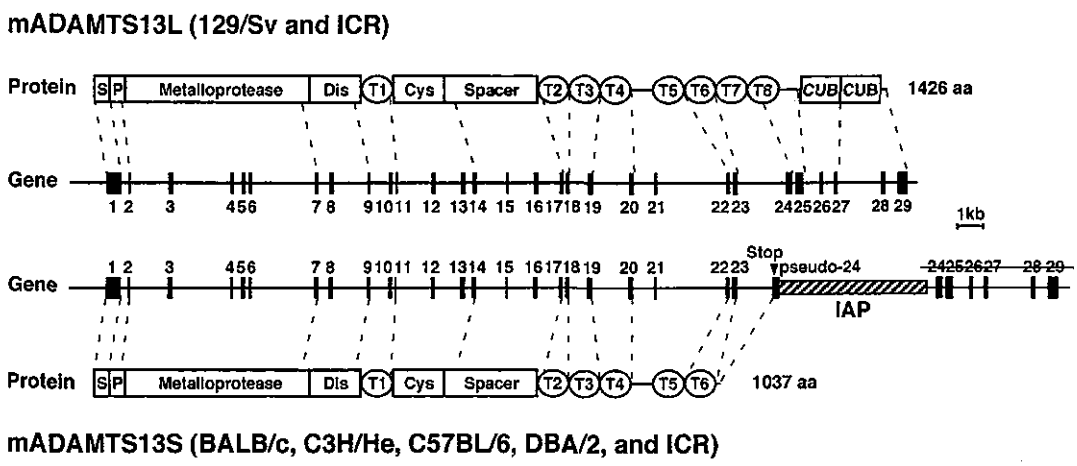

FIG. 5. **Schematic structure of two forms of the *Adamts13* genes and proteins.** Genomic and protein structures of mADAMTS13L in the 129/Sv strain and of mADAMTS13S in the BALB/c, C3H/He, C57BL/6, and DBA/2 strains are shown. The outbred ICR strain has both type alleles. The exons and introns are drawn to scale. A *hatched box* represents the IAP insertion in intron 23. *S*, signal peptide; *P*, propeptide; *Dis*, disintegrin-like domain; *T1–T8*, thrombospondin type1 motifs; *Cys*, cysteine-rich domain.

jected to Western blot using a rabbit anti-GST antibody (Molecular Probes) and an HRP-labeled goat anti-rabbit IgG antibody (Kirkegaard & Perry Laboratories) as described (24). We also analyzed the proteolytic activity of plasma from five mouse strains in the same way.

RESULTS

Identification of Adamts13 in the C57BL/6 Strain—To identify the orthologous mouse gene of human *ADAMTS13*, we performed a BLAST search in the public data base, based on the human *ADAMTS13* cDNA sequence (GenBank™ accession number AB069698, 4,284-nucleotide ORF) reported by Soejima *et al.* (8). This search led us to identify a compatible genomic sequence (GenBank™ accession number AC090008) derived from the C57BL/6 strain. This sequence was located on chromosome 2, band A3 and contained 29 conserved exons similar to human *ADAMTS13*. To obtain the cDNA to corresponding mRNA, we performed RT-PCR and 3′-RACE using poly(A)$^+$ RNA from the liver of a C57BL/6 mouse. Unexpectedly, the cDNA sequence (GenBank™ accession number AB071302) included only a 3,114-nucleotide ORF derived from 24 exons.

From a comparison between the cDNA and the genomic sequences of the C57BL/6 strain, we found a 6-kb retrovirus-like sequence in intron 23 of the *Adamts13* gene (Fig. 1). This sequence was flanked by the identical 338-bp sequence with a 6-bp (CACTAG) duplication of target site, as is often observed for retrotransposition. A BLAST search identified the insertional element as an intracisternal A-particle (IAP), which is one of the retrotransposons present at about 2,000 sites in the mouse genome (26). This insertion of IAP seemed to be responsible for loss of the original mRNA 3′-end by splicing exon 23 to pseudo-exon 24 that contains a premature stop codon.

Identification of Adamts13 in the 129/Sv Strain—To determine whether the IAP insertion into the *Adamts13* gene is common to a variety of mouse strains, we carried out PCR genotyping of five inbred and one outbred strains (Fig. 2*A*). A mixture of three primers was used for the reaction; Primers F and R1 were designed to produce a 305-bp band in the absence of IAP, and primers F and R2 were designed to produce a 230-bp band in the presence of IAP. This experiment revealed that the IAP insertion was present in the BALB/c, C3H/He, and DBA/2 strains but not in the129/Sv strain (Fig. 2*B*). The outbred ICR strain was genetically heterogeneous with respect to the IAP insertion into the *Adamts13* gene. Southern blot analysis using probes upstream of the IAP target site revealed that *Adamts13* was a single copy gene and confirmed the strain-specific insertion of IAP (Fig. 2*C*). These results implied that the *Adamts13* gene transcript of the 129/Sv mice and some ICR mice might contain residual exons lost in the other mouse strains.

To confirm this hypothesis, RT-PCR was performed using liver poly(A)$^+$ RNA from a 129/Sv mouse. The obtained sequences indicated that the *Adamts13* cDNA (GenBank™ accession number AB112362) contained a 4,281-nucleotide ORF similar to human *ADAMTS13* (4,284-nucleotide ORF). To determine the complete genomic sequence of *Adamts13* in the 129/Sv strain, we screened a 129/Sv mouse λ genomic library. Sequence analysis of positive phage clones confirmed the absence of IAP in the *Adamts13* gene. *Adamts13* in the 129/Sv strain (GenBank™ accession number AB095445) contained 29 exons like human *ADAMTS13* and spanned ~30 kb.

To examine the effect of IAP on *Adamts13* mRNA splicing, RT-PCR was performed using liver poly(A)$^+$ RNA from six mouse strains (Fig. 3). The exon 21/22-specific sense primer, the exon 24/25-specific antisense primer, and the pseudo-exon 24-specific antisense primer were mixed and used for the amplification. We detected the IAP chimeric transcript in four inbred strains with the IAP insertion. In contrast, the IAP-free transcript was observed in the 129/Sv strain. The heterogeneous expression of two types of transcripts was observed in samples from the ICR strain. To characterize the transcripts in more detail, Northern blot analysis of liver RNA was carried out using a 1.3-kb probe spanning exons 3–13 of *Adamts13* cDNA (Fig. 4*A*). The RNA was prepared from the same animals as used for the Southern blot analysis. An ~3.5-kb mRNA corresponding to the size of IAP chimeric transcript was detected in the C57BL/6 and the ICR strains. The IAP-free transcript of ~5.0 kb was observed in the 129/Sv and the ICR strains.

Thus, these results clearly indicate the presence of two types of mouse *Adamts13* in a strain-specific manner (Fig. 5). *Adamts13* of the 129/Sv strain encodes an ADAMTS13 protein containing 1,426 amino acid residues with the same domain structure as hADAMTS13, designated mADAMTS13L. *Adamts13* of the BALB/c, C3H/He, C57BL/6, and DBA/2 strains encodes the shorter ADAMTS13 protein including only 1,037 amino acid residues, designated mADAMTS13S. In this protein, the C-terminal two TSP1 and two CUB domains are replaced with the 16-amino acid sequence, ALVWEAAPTFAVTRWR, derived from the IAP. The outbred ICR strain carries either the IAP-free or IAP-inserted allele or both.

Expression of the Adamts13 mRNA in Mouse Tissues—To study the expression pattern of the mouse *Adamts13* gene, we analyzed Northern blots containing poly(A)$^+$ RNA from various tissues of the BALB/c and the Swiss Webster strains. As shown